Modeling how and why aquatic vegetation removal can free rural households from poverty-disease traps.

Molly J Doruska[a], Christopher B Barrett[a,b], Jason R Rohr[c]

[a] Charles H. Dyson School of Applied Economics and Management, Cornell University, Ithaca, NY, USA

[b] Jeb E. Brooks School of Public Policy, Cornell University, Ithaca, NY, USA

[c] Department of Biological Sciences, Environmental Change Initiative, Eck Institute of Global Health, University of Notre Dame, Notre Dame, IN, USA

Corresponding Author: Christopher B. Barrett, cbb2@cornell.edu

Author Contributions: MD performed the literature search, data curation, model development, formal analyses, figure development, and contributed to writing the manuscript. CB and JR conceptualized the project, secured funding, directed the project and analyses, assisted with model development and helped write and revise the manuscript.

Competing Interest Statement: The authors declare no competing interests.

Keywords: Agricultural households, bioeconomic modeling, fertilizer, Schistosomiasis, Senegal

September 2024 revision

1 **Abstract**

2 Infectious disease can reduce labor productivity and incomes, trapping subpopulations in a
3 vicious cycle of ill health and poverty. Efforts to boost African farmers' agricultural production
4 through fertilizer use can inadvertently promote the growth of aquatic vegetation that hosts
5 disease vectors. Recent trials established that removing aquatic vegetation habitat for snail
6 intermediate hosts reduces schistosomiasis infection rates in children, while converting the
7 harvested vegetation into compost boosts agricultural productivity and incomes. We develop a
8 bioeconomic model that interacts an analytical microeconomic model of agricultural households'
9 behavior, health status and incomes over time with a dynamic model of schistosomiasis disease
10 ecology. We calibrate the model with field data from northern Senegal. We show analytically and
11 via simulation that local conversion of invasive aquatic vegetation to compost changes the
12 feedback among interlinked disease, aquatic and agricultural systems, reducing schistosomiasis
13 infection and increasing incomes relative to the current status quo, in which villagers rarely
14 remove aquatic vegetation. Aquatic vegetation removal disrupts the poverty-disease trap by
15 reducing habitat for snails that vector the infectious helminth and by promoting production of
16 compost that returns to agricultural soils nutrients that currently leach into surface water from on-
17 farm fertilizer applications. The result is healthier people, more productive labor, cleaner water,
18 more productive agriculture, and higher incomes. Our model illustrates how this ecological
19 intervention changes the feedback between the human and natural systems, potentially freeing
20 rural households from poverty-disease traps.

21 **Significance Statement**

22
23 We connect a disease ecology model of schistosomiasis infection dynamics to an analytical
24 microeconomic model of agricultural households optimally choosing behaviors subject to
25 environmental and market constraints. By rooting the poverty-disease trap in a structural model of
26 household decision-making, and by introducing a model of natural dynamics into an economic
27 model, we integrate parallel literatures, providing a foundation for more precise exploration of the
28 structural underpinnings of poverty-disease traps based on human-nature interactions. This
29 analytical model also provides a theory-based, numerical, and structural explanations for why a
30 novel ecological intervention to clear aquatic vegetation from water points succeeds in
31 dramatically reducing schistosomiasis infection rates while boosting agricultural productivity.
32
33
34
35
36

Main Text

Introduction

Rural populations in low and middle income countries suffer relatively high infectious disease prevalence and low agricultural productivity, which jointly result in low incomes that can reinforce those conditions, resulting in a poverty-disease trap.[1-11] Efforts to intensify agricultural production and break out of the trap too often fail when inadequate attention is paid to how human behaviors interact with the dynamics of the natural ecosystems that support rural peoples' livelihoods, for example, when increased fertilizer use inadvertently aggravates infectious disease exposure.[12,13] Sustainably improving the livelihoods of millions of poor rural people requires structural understanding of the potential feedbacks among agricultural production, disease ecology, and rural households' behaviors and well-being.

One example of a poverty-disease trap involves schistosomiasis, a neglected tropical disease that currently infects more than 200 million people around the globe, with 800 million people at risk of infection.[14-16] Schistosomiasis is caused by a snail-hosted flatworm. Snails infected with schistosomes inhabit aquatic plants in freshwater habitats (lakes, rivers, even irrigation canals). These snails release larval schistosomes into the water, which then penetrate the skin while people perform daily activities, like bathing, washing clothes or swimming.[17,18] Adult worms settle in the veins surrounding the gastrointestinal (*Schistosoma mansoni*) or urinary (*Schistosoma haematobium*) tract of infected individuals. The eggs released by the worms trigger chronic inflammatory responses causing several ailments including, but not limited to, loss of tissue function, resulting in reduced physical energy – and thus labor supply– among adults and stunted growth and learning deficits among children.[19-21] Conventional methods to control schistosomiasis rely on mass deworming, whereby all children and/or adults within a village receive deworming medication to clear current infections. Mass deworming does not, however, clear snails and schistosomes from the water sources, thus reinfection occurs quickly, typically within a few months.[22,23] While mass deworming can generate large, transitory reductions in human infection levels, reducing long-term cycles of schistosomiasis infection and reinfection requires strategies that target the structural sources of the infection cycle.[22-27]

Recent field trials revealed that schistosomiasis in schoolchildren can be significantly reduced by removing aquatic vegetation that serves as the habitat for snail intermediate hosts, complementing infection control through deworming.[13] Researchers converted this aquatic vegetation into compost and livestock feed, which increased agricultural production and lowered agricultural input costs. Aquatic vegetation removal for joint infectious disease control and the production of agricultural inputs is not currently widely practiced in the northern Senegal study region or elsewhere. Furthermore, *Ceratophyllum demersum*, the keystone aquatic vegetation species of interest in this model, is found throughout Africa and on every continent with endemic schistosomiasis.[18] Therefore, the aquatic vegetation removal model might apply to settings throughout the developing world, potentially benefitting millions who suffer from schistosomiasis infection. Recent findings also suggest that targeting snails, such as through aquatic vegetation removal, is the most effective way to reduce schistosomiasis transmission.[13,28] It is therefore important to understand why this practice works and whether it might offer a transferable method for escaping from poverty-disease traps by offering households an economic incentive to remove aquatic vegetation, thereby reducing schistosomiasis exposure while simultaneously boosting agricultural productivity and household incomes.

We develop a bioeconomic model to examine the relationship among agricultural production, poverty, and disease in northern Senegal and to explore if and why aquatic vegetation removal can break poverty-disease traps as part of a community-based adaptation measure.[29] We start with a classic non-separable microeconomic model of agricultural household behavior[30] and connect it to a disease ecology model of schistosomiasis dynamics,[28] linking the models through

91   household decisions about labor allocation, aquatic vegetation harvest, and fertilizer application,
92   decisions that affect both agricultural outcomes and the underlying aquatic ecosystem and
93   thereby (indirectly) the probability of human infection (figure 1). Existing macro-scale models of
94   poverty-disease traps necessarily abstract away from individual-level incentives and
95   behaviors,[5,8,9] relying on reduced form associations at the population scale. We instead follow a
96   tradition of structural microeconomic models that explicitly link human behaviors to the dynamics
97   of natural phenomena.[31-34] A structural microeconomic model enables us to identify the conditions
98   under which households might voluntarily undertake aquatic vegetation removal, those under
99   which vegetation removal may suffice to control schistosomiasis transmission, and how such
100   incentives and outcomes vary with household attributes, such as farm size.

102   Our results highlight two key feedback loops households face. First, under the status quo, with no
103   aquatic vegetation removal, we see explicitly how a poverty-disease trap emerges. Vegetation
104   growth remains unchecked by households, boosting schistosomiasis infection rates that reduce
105   household labor supply, which in turn reduces the time allocated to agricultural production and
106   thus overall incomes. Low incomes and high prevalence of infectious disease co-exist under this
107   regime. If, however, households implement a very simple intervention, clearing the water access
108   point of invasive weeds that host the snails that vector the schistosomes, infections plummet and
109   labor supply, agricultural productivity and incomes increase, yielding both higher incomes and
110   lower disease prevalence, thus helping to break the poverty-disease trap.

112   Second, fertilizer runoff provides key nutrients that foster aquatic plant growth, reducing the
113   effectiveness of aquatic vegetation removal and thereby allowing snails and infection to persist.
114   This makes it more challenging for households to break the poverty-disease trap where steady
115   state income below (above) the income-or-expenditures-based poverty line implies being in (out
116   of) a poverty trap.[3] This reveals an under-recognized tradeoff in agricultural development efforts;
117   while fertilizer use increases agricultural output, it can also indirectly promote infectious disease
118   exposure, with analytically ambiguous effects on health, incomes and living standards, much like
119   pesticides.[35] Together, these main results demonstrate the importance of understanding and
120   considering structural feedbacks when proposing interventions to improve livelihoods and enable
121   escapes from poverty-disease traps.

Results

126   When households do not harvest the aquatic vegetation, the vegetation remains stable at the
127   system's carrying capacity (figure 2A). Because the snail vector population scales with the
128   vegetation that provides it habitat and nutrients, household infection reaches a high steady state
129   (figure 2B, C). Households spend most labor on their farm and use moderate amounts of fertilizer
130   in food production. High infection rates limit labor supply, however, leading to low income and a
131   poverty-disease trap. These patterns are very similar across the wealth distribution.

133   If the household can harvest aquatic vegetation, however, all household types allocate only a
134   small fraction of their labor to that task, but with considerable impact. Households' clear some
135   vegetation from the water source, leading to a stable vegetation level well below the carrying
136   capacity, consistent with field experimental data finding that 10 or fewer individuals could clear a
137   village's water access points in a day.[13] Even with continued household fertilizer use, modest
138   effort allocated to aquatic vegetation harvest maintains a reduced aquatic vegetation stock,
139   driving down the household infection rate, especially for villages characterized by poorer
140   households with low or moderate land endowments (figure 2D). The differences between villages
141   with smaller farms and poorer households versus larger farms and relatively richer households in
142   this setting are driven by differences in optimal fertilizer use. Higher incomes relax households'
143   budget constraints, permitting increased fertilizer purchases, given that the expected marginal
144   revenue product of fertilizer significantly exceeds its price in this setting, at prevailing application

145 rates. But more fertilizer use results in increased runoff, resulting in slightly higher levels of
146 aquatic vegetation and thus schistosomiasis infection rates for villages with larger farms and
147 better-off households.
148
149 Most household labor remains allocated to food production, but lower infection rates mean
150 greater labor availability. This greater labor, in addition to the added nutrients returned to the soil
151 from the compost, leads to higher median incomes than in the baseline case without vegetation
152 harvest (figure 2E). These results highlight that the attractive economic returns to compost
153 created from the harvested aquatic vegetation[13] can help disrupt disease ecology dynamics, both
154 reducing infection rates and boosting incomes in a favorable reinforcing feedback loop. The
155 model helps us understand the underlying mechanisms that explain how and why the intervention
156 seems to work.
157
158 Fertilizer use is higher when vegetation is harvested. Since compost and fertilizer are substitutes,
159 one might expect fertilizer use to decrease as farms begin harvesting aquatic vegetation. But
160 such substitution effects are often dominated by income effects, especially when fertilizer use is
161 suboptimal relative to its expected profitability due to farmers' financial liquidity constraints, as the
162 prior household modeling literature has long established.[31,32,36] Aquatic vegetation harvest
163 increases incomes by increasing household labor availability and food productivity. Those higher
164 incomes then stimulate greater household food demand and relax financial liquidity constraints to
165 fertilizer purchase. So long as the expected returns to fertilizer use significantly exceed the price
166 of fertilizer, as seems true in the northern Senegal context, then farmers apply fertilizer if they can
167 afford it, Thus, the income effect can be – and as parameterized based on the available data from
168 this context, is – stronger than the substitution effect and fertilizer use increases as farmers
169 compost harvested aquatic vegetation. The higher dynamic equilibrium of greater food production
170 and incomes alongside lower infection rates gest sustained by farmers regularly devoting some of
171 their increased labor availability from lower infection rates to clearing water access points.
172
173 Our simulations are consistent with the empirical association of fertilizer use with infectious
174 disease exposure.[12,13] The optimal level of fertilizer for a household may depend on the level of
175 infection. To test this directly, we re-ran the simulations starting with households at different
176 infection rates and keeping all other model parameters the same. We calculated the median
177 optimal first-year fertilizer use and plotted it across the different starting infection conditions
178 (figure 3). Optimal fertilizer use is negatively associated with infection rate, as predicted. The
179 decrease is meaningful in magnitude; very high infection levels are associated with almost a 50%
180 decrease in optimal fertilizer use compared with low infection levels This result again reinforces
181 the central point that some innovation is needed to break communities out of their current high
182 schistosomiasis infection, low agricultural productivity equilibrium.
183
184 We explore the sensitivity of our results to the effect of fertilizer runoff on vegetation (ρ), the
185 vegetation recolonization rate ($n0$), the vegetation growth rate (r), and the price of fertilizer (p_u).
186 We also conduct a sensitivity analysis of the price of the household good (p_h).[*] For the sensitivity
187 analysis, we focus on changes to parameters in the system and consider the median household
188 land holding of two hectares.
189
190 The core model results described above are generally robust to changes in the effects of fertilizer
191 runoff on vegetation growth, recolonization rate, and growth rate, and economic incentives
192 modeled through changes in the price of fertilizer and the household good. Slightly higher levels
193 of infection and lower labor availability result when the fertilizer runoff effect (figure 4) and
194 vegetation recolonization rate increase (figure S1). At lower levels of vegetation growth, the

---

[*] The ratio of prices governs the economic incentives households face, so changing the price of the household good implicitly changes the relative value of food.

195   vegetation stock is smaller, infection prevalence is lower, household labor availability is higher,
196   and income is slightly improved (figure 5).
197
198   As expected, cheaper fertilizer leads households to use more of it, which results in modest
199   increases in infection prevalence (figure S2). Finally, our results show no meaningful changes
200   when the price of the household good changes (figure S3). Together, these results show that the
201   patterns in our main results are consistent across a range of reasonable values for underlying
202   agroecosystem and market conditions, and thus provide a robust structural way to capture the
203   relationship between aquatic vegetation growth, the microeconomic decisions of households, and
204   poverty and disease outcomes. The returns to compost in food production are routinely large
205   enough to induce aquatic vegetation harvest if people are aware of the household benefits.
206   However, the impact of aquatic vegetation harvest can be muted at higher levels of fertilizer use
207   because vegetation growth spurred by fertilizer use offsets some of the gains made by harvesting
208   aquatic vegetation.
209
210   Back-of-the-envelope estimates suggest that economic gains from universal awareness of the
211   potential benefits from aquatic vegetation harvest could average at least 3,200 USD per village or
212   3.25 USD per person annually, perhaps double that if one includes the estimated long-term
213   earnings gains from improved child health and education. These are modest but significant gains
214   for poor, rural communities. The estimated regional gain from aggregating across all villages in
215   West Africa within five kilometers of surface freshwater that are likely to host the vegetation,
216   snails and schistosomiasis is 138.5 million USD per year.
217
218   **Discussion**
219
220   We developed a micro-structural model of a poverty-disease trap by linking a non-separable
221   agricultural household model to one of schistosomiasis disease ecology dynamics through
222   household labor availability, labor allocation choices, and optimal fertilizer use. The household-
223   centered approach allows us to analyze how poverty-disease traps can exist under current
224   conditions and how and why simple, low-cost interventions like aquatic vegetation harvest can
225   help break those traps. Under the status quo, without aquatic vegetation harvest, infection
226   prevalence is consistently high and household labor availability and income are steadily low.
227   When we allow for vegetation harvest in the model, simulating what might happen after an
228   agricultural extension and public health information campaign to promote aquatic vegetation
229   removal, we see consistently lower infection levels and higher incomes. Introducing aquatic
230   vegetation removal to this single equilibrium poverty trap model induces different household
231   decisions that can lead to higher dynamic equilibrium incomes. The effect of aquatic vegetation
232   harvest is greater in combination with measures that reduce nutrient runoff that spurs aquatic
233   vegetation regrowth. Continued household fertilizer use limits the gains for those with the highest
234   land holdings, signaling that this seems an intervention especially well-suited to communities with
235   smaller farms. Thus, aquatic vegetation harvest has the potential to allow households to reduce
236   the cycle of schistosomiasis infection and reinfection that characterize the poverty-disease traps
237   currently confronting many rural households in northern Senegal, and many other communities in
238   the low-income tropics.
239
240   While removed aquatic vegetation can be dried and used for animal feed or used as a feedstock
241   for biodigesters in producing off-grid energy, economic analyses in our study setting indicate that
242   compost is the first-best use among the options evaluated by researchers.[13] Preliminary results
243   suggest that a latent market for compost (and livestock feed) exists.
244
245   One limitation of our modeling strategy is that we only explore the representative household's
246   choices, but water sources and water access points serve many households at one time. In the
247   case of fertilizer use, one household's decision to use lots of fertilizer will inevitably impact the
248   common water source, increasing the aquatic vegetation and schistosomiasis reservoir for all

249   households who use that water source. This provides an opportunity for households to harvest
250   more vegetation, but it also poses a greater infection risk due to other households' decisions. A
251   natural extension of the current model would build out these interhousehold and spatial
252   interactions into a dynamic general equilibrium bioeconomic model to trace out within-village
253   spillover effects. Our results suggest that differential fertilizer use – and perhaps differential water
254   contact rates – is an important piece of the system. Documenting these village externalities may
255   prove helpful to fully understanding and tackling the poverty-disease trap.
256
257   Additionally, our representative household model does not account for any growth in a household
258   or village over time. In the more general case of bioeconomic modeling of infectious disease
259   transmission, one might worry about habitat changes affecting the transmission patterns.[37] With
260   aquatic vegetation removal, villagers are unlikely to create new fresh surface water habitats for
261   snails as the rivers, lakes, and irrigation canals are relatively fixed over time and space. The snail
262   habitat within the aquatic system is endogenous to the model as we directly model the amount of
263   aquatic vegetation or snail habitat with the system. In our setting, we model aquatic vegetation
264   removal, a form of habitation conversion that reduces the likelihood of contact between the
265   disease hosts and humans. Furthermore, nutrient runoff is the key driver of snail habitat, and we
266   explicitly link fertilizer use to aquatic vegetation in the model. We could consider increased
267   cultivated land over time, which would be equivalent to adding a positive time trend to fertilizer
268   use to the model. In northern Senegal, it is unclear if cultivated land is expanding and thus we
269   hold land constant. If cultivated land increased, households would need to more frequently
270   remove aquatic vegetation to reduce schistosomiasis exposure.
271
272   Climate change and biodiversity loss may also influence the link between schistosomiasis and
273   aquatic vegetation removal.[38] Temperature does impact schistosomiasis transmission.[39] Rising
274   global temperatures may therefore alter the relationship between aquatic vegetation removal and
275   schistosomiasis infection over our 20-year time horizon. While we abstract away from the impact
276   of rising temperatures and other drivers of global change in this model, future work should
277   explore how external drivers could interact with current feedback loops within human and
278   environmental systems.
279
280   Field trials to date do not detect any significant ecological damage from aquatic vegetation
281   removal.[13] Unlike malaria control efforts, such as removing mangroves,[40] aquatic vegetation
282   removal is currently highly localized and requires only removing vegetation in the immediate
283   vicinity of water access points. Most of the river or lake environment is untouched. Even so,
284   ongoing work is explicitly monitoring for unintended ecological damage as this intervention
285   scales.
286
287   While this model focuses on understanding how and why this intervention works in the specific
288   context of the Saint Louis and Louga regions in northern Senegal, the modeling approach and
289   principles of the intervention we evaluate likely apply to other settings with endemic infectious
290   diseases. In fact, our back-of-the-envelope calculations scaled the benefits to all of west Africa,
291   assuming that the benefits of aquatic vegetation removal observed in Senegal are similar in other
292   locations. The estimated regional gain from aggregating across all villages in West Africa is 138.5
293   million USD per year. Note that these gains arise just from the value of the direct productivity
294   effects of using the harvested aquatic vegetation to boost soil nutrients and thus agricultural
295   output and the added earnings from fewer workdays lost to illness. This estimate is likely quite
296   conservative in that it abstracts away from the longer-term earnings gains arising from improved
297   health and educational attainment of children from reduced schistosomiasis infection.[41-44] In fact,
298   our per person annual gain in earnings is similar to estimates of the longer-term estimates of
299   earnings gains from deworming, even without accounting for spillover gains on untreated
300   children.[43] Given that aquatic vegetation removal has similar gains as deworming,[13] one might
301   reasonably hypothesize that adding these long-term earnings gains among children to the nearer-
302   term gains arising from vegetation removal and conversion into compost roughly doubles the

303 long-run estimated benefits. Additionally, we identify and structurally model a key potential
304 mechanism to reduce infectious disease burdens in the low-income tropics, demonstrating the
305 importance of understanding feedback loops between household economic decision making and
306 the underlying natural environment, which has applications to other neglected tropical diseases
307 and to other complex relationships between human and environmental systems. Consequently,
308 we hope that the empirical calibration of our integrated human–biological–socioeconomic model
309 provides a framework to evaluate environmental interventions to control other vector-borne
310 diseases, such as malaria, Chagas disease, African Trypanosomiasis, or Leishmaniasis.
311
312 Poverty-disease traps are widespread, thus understanding solutions is important. Research in
313 Kenya finds significant impacts of deworming on child learning and that of their siblings[41,42] and
314 labor market outcomes later in life after deworming.[43,44] Thus, there are likely large potential long-
315 term benefits of aquatic vegetation removal not modeled nor discussed here given the twenty-
316 year time horizon we impose in the modeling. Policy makers, community leaders and
317 development agencies should consider aquatic vegetation removal as an effective form of
318 schistosomiasis infection control that can also boost incomes and overall quality of life for millions
319 of people.
320
321
322 **Materials and Methods**
323
324 The bioeconomic model has two submodels. The first describes the disease ecology dynamics,
325 more specifically, how the schistosome, aquatic vegetation, and snail populations interact, and
326 relates these populations to human infections. The second, an agricultural household submodel,
327 describes how utility maximizing households make decisions about how to allocate their land,
328 labor, and income. We describe the key parameters and model equations here. A full description
329 of the model with equations can be found in SI Appendix Text S2.
330
331 The household's problem is a variant of the non-separable agricultural household model in which
332 consumption and production decisions become inextricably linked by multiple market failures that
333 typically characterize poor rural villages like those in our setting.[30] The economic model begins
334 with a representative household that maximizes utility, defined over consumption of food, an
335 aggregate non-food household good, leisure, and the health status of household members. We
336 assume that utility is well-defined, increasing and concave in all its arguments. We model the
337 household's nutrient intake via food consumption. The health production function is Cobb-
338 Douglas for food consumption and the fraction of household members infected downscales the
339 health status variable as the fraction infected increases. Health status increases with food
340 consumption, representing the value of more nutrient intake. The household can only influence
341 health status through more food consumption or a lower infection prevalence; one cannot buy
342 good health. Because aquatic vegetation is a common pool resource, there is no market for
343 aquatic vegetation, either in the water or as harvested vegetation. The multiple market failures in
344 health status and aquatic vegetation together create non-separability between the household's
345 production and consumption decisions. To simplify the model, we also assume no market exists
346 for land rentals or sales and from cash labor markets as land or labor transactions are uncommon
347 in the study area. Households allocate their time among cultivating food, harvesting aquatic
348 vegetation, and leisure and commit their land to their own agricultural production. These
349 assumptions do not qualitatively change model outcomes.
350
351 If households choose to harvest aquatic vegetation, they turn it into compost, which increases
352 agricultural productivity.[13] Households produce food using land, labor, fertilizer, and compost from
353 harvested aquatic vegetation. Recent experimental evidence finds that compost and urea fertilizer

354   are virtually perfect substitutes.[13] Harvesting vegetation only requires labor.[†] The household
355   employs a constant elasticity of substitution (CES) food production function while aquatic
356   vegetation harvest follows Cobb-Douglas production technology.[‡] More details on the agricultural
357   household model are in the supplementary materials.

359   To simulate the status quo ex ante, we also present a simplified version of the model without
360   aquatic vegetation harvest, in which households cannot use labor to harvest aquatic vegetation to
361   produce compost. Our core comparisons thus simulate the equilibrium effects of making villagers
362   aware of the prospective value of composting harvested aquatic vegetation.

364   The disease ecology model tracks the populations of aquatic vegetation (*Ceratophyllum*, N),
365   miracidia (larval schistosomes that infect snails, M), infected and susceptible snails (I_2 and S_2),
366   cercariae (larval schistosomes that infect humans, P), and infected and susceptible humans
367   (I_1 and S_1). We adapt an existing schistosomiasis disease ecology model[26] to fit the Senegalese
368   context and down-scale the parameters from a large community to one that matches the
369   household-level simulations. Additional details on the disease ecology model are in the
370   supplemental materials.

372   Relative to the human lifespan, the schistosomiasis infection cycle is relatively short. Cercariae
373   live around 10 hours, miracidia live around 25 hours, and snail infections last around 100 days.[45]
374   Very few or none of the existing cercariae or miracidia population will survive over the course of
375   the year, which creates a challenge to match timescales across the household and disease
376   ecology submodels. One could convert the continuous time disease ecology submodel to discrete
377   time to match the household submodel through significant linearization and assumptions about
378   annual changes in miracidia, cercariae, and snail populations. But that can cause meaningful
379   aggregation errors. We therefore instead use a continuous time disease ecology submodel that
380   better matches the timeline of the schistosomiasis infection cycle. We simulate annual changes
381   by simulating the system of differential equations forward 365 days, where all parameters are
382   given in daily rates. We then export the annual output to the discrete time household model that
383   operates at annual time steps.

385   Furthermore, we could instead model household decisions on a smaller timescale to match the
386   disease ecology submodel.[5,46] However, we explicitly want to model agricultural households
387   making decisions over an entire cropping season. Thus, we use an annual household model to
388   best capture the microeconomic decisions that are the foundation of our model.

390   The disease ecology submodel and the household submodel link to one another in two ways.
391   The first is through the infection status of the household, which directly affects household utility
392   and impacts the household's labor availability and thus income and the budget set that constrains
393   purchase of fertilizer as well as food and consumption goods. The second is through the
394   household's use of urea fertilizer and its aquatic vegetation harvest, each of which changes the
395   vegetation population within the water source. Thus, infection status can affect income, which in
396   turn can affect fertilizer use and runoff that fuels aquatic vegetation growth.

398   The disease ecology submodel provides population estimates of infection, which we scale down
399   to individual- and household-level infection rates through stochastic infection realizations drawn
400   from an independent Bernoulli distribution for each household member at the start of each time
401   period. The distribution's mean is the infection rate predicted by the disease ecology submodel,

---

[†] While it requires a pit to convert vegetation into compost, we assume there exists sufficient
unused, free land within the village such that land availability does not constrain compost
production.
[‡] Labor is the only input to harvest vegetation, so there is no need for a CES specification to allow
for substitution among inputs.

402   the population infection prevalence. After the first period, we also take random draws for curing
403   infection, where the mean of the Bernoulli random variable was set at 0.25, which captures the
404   fact that households in this region experience sporadic mass deworming campaigns.[47] The lack
405   of smooth time paths in labor availability and household infections (figure 2) arises from the
406   stochastic process that generates household infections and periodic deworming within the model.
407
408   Since each individual household is only one small part of a village and villages only access a
409   small portion of the entire aquatic system, these households do not individually influence the
410   disease ecology submodel. Since household behavior does not individually impact disease
411   ecology, the household does not consider the equations of the disease ecology submodel in its
412   own optimization. In this way, the household solves a series of static, single period optimization
413   problems as in prior bioeconomic models.[31,§] In this framework, the disease ecology submodel
414   shows how the state and the average infection rate change over time. In each period, we solve
415   the household's static optimization problem and then use the household's choices to determine
416   the stock of aquatic vegetation and the realizations of infection to determine the current infection
417   prevalence. With these new starting populations, we simulate the disease ecology model one
418   year forward to give the state of infection in the next time period. The model is then solved by the
419   following iterative process for each period in the simulation:
        1. We use Bernoulli random draws to realize household infection;
        2. The household solves their static problem by allocating its time and money to
             maximize its period-specific utility;
        3. Using the realizations of infection and the household's decisions, we calculate the
             current aquatic vegetation population and the current number of infected and
             susceptible individuals. We use these starting values and simulate the disease
             ecology submodel forward one year and calculate the vegetation population and
             village infection rate in the following period;
        4. Repeat from step one for 20 annual periods.
429   Additional details on the linkages between submodels are in the supplemental materials.
430
431   We limit simulations to 20 years to explore the within-generation results of the model to see what
432   happens when aquatic vegetation harvest is introduced, in particular, if vegetation harvest
433   becomes a sustained behavior, resulting in new levels of (reduced) equilibrium infections and
434   (higher) household incomes. This time frame is long enough to capture any short-term changes in
435   the equilibrium level of schistosomiasis infection but allows us to abstract away from long-term
436   changes, including through impacts on children's educational attainment, or in human fertility
437   behaviors that would further complicate the model.
438
439   We simulate the model in Julia 1.6.2 and aggregate and analyze the model output in Stata 16.
440   For each household type, we conduct 1,000 stochastic simulations to capture different optimal
441   paths based on the realized random infection draws. Household types are determined by land
442   holdings, which are set at the 25th, 50th, and 75th percentiles of land holdings in the Saint Louis
443   and Louga regions based on the Harmonized Survey on Household Living Standards in Senegal
444   2018-2019 (table S1).[48] Land holdings are proxies for wealth in this context and these
445   simulations. Comparisons across land holding types give insight into how wealth levels impact the

---

§ Any of several justifications exist to follow this approach. Households cannot fully control the
decisions of all household members, such as parents telling their children to stay out of the water
but children not listening, thus the natural dynamics escape household control. Or households
might not fully understand the evolution of the disease ecology submodel as given in the
equations that connect vegetation, miracidia, cercariae, snails, and humans. Each of these is
likely true to some degree, allowing us to avoid the unrealistic and computationally task of
modeling a household that monitors all seven populations in the disease ecology submodel as
state variables. That would require significant discretization or a large reduction in the number of
states to solve given the curse of dimensionality in optimal control problems.

optimal decisions of the household. We track the following key outcome variables: household labor availability, labor allocated to food production, leisure, fertilizer use, the vegetation load in the water source, the household's level of infection, and the household's income. We then take the median of 1,000 simulations for each outcome at each time period for each household land endowment.

To begin, we eliminate the household's option to remove vegetation and produce compost by mechanically setting the marginal product of labor in aquatic vegetation harvest to zero. This lets us model how households currently behave and establish starting levels of infection and income under current conditions.

After solving the model and running the simulations described above, we generate back-of-the-envelope estimates of the net income gains from aquatic vegetation removal at scale. We emphasize the many strong simplifying assumptions in these estimates, which are meant to give a sense of the magnitude of the prospective gains from diffusing aquatic vegetation removal broadly across West Africa.

To generate those estimates, first we calculated the difference in median income with and without aquatic vegetation removal for each of our representative households after five years of vegetation removal. Then, we scaled these estimates to the village level. We assume that villages have 985 people (the average village size for this region for villages within five kilometers of a water source)[49-51] with an average household size of 10, so on average 98.5 households. Then, we assume that the 0.5, 2.0, and 5.5 hectares households represent 25%, 50% and 25% of total households in the average village, respectively, enabling us to scale up to village level the median increase in household income from aquatic vegetation removal conditional on land holdings. At year five, aquatic vegetation removal produces estimated additional average income gains of 3,197 USD per village per year. These estimates assume that all households know about aquatic vegetation removal and the potential economic benefits from making compost.

Finally, we used remote sensing imagery analysis to scale to all of West Africa. We estimate that there are 43,320 villages across West Africa that are within five kilometers of surface freshwater and likely to host the vegetation, snails and schistosomiasis.[49-51] This number was then multiplied by the estimated net gains per village estimated from Senegal.

A replication package with the code and data used is available at https://github.com/mdoruska/Bioeconomic_Model.

Acknowledgments

References

498   1. C. B. Barrett, M. R. Carter, The economics of poverty traps and persistent poverty:
499   Empirical and policy implications. *Journal of Development Studies* **49**, 976–990 (2013).
500   2. C. B. Barrett, *et al.*, Welfare dynamics in rural Kenya and Madagascar. *Journal of*
501   *Development Studies* **42**, 248–277 (2006).
502   3. C. B. Barrett, T. Garg, L. McBride, Well-being dynamics and poverty traps. *Annual*
503   *Review of Resource Economics* **8**, 303–327 (2016).
504   4. C. B. Barrett, M. R. Carter, J.-P. Chavas, M. R. Carter, *The Economics of Poverty Traps*
505   (University of Chicago Press Chicago, 2019).
506   5. M. H. Bonds, D. C. Keenan, P. Rohani, J. D. Sachs, Poverty trap formed by the ecology
507   of infectious diseases. *Proceedings of the Royal Society B: Biological Sciences* **277**,
508   1185–1192 (2010).
509   6. M. R. Carter, C. B. Barrett, The economics of poverty traps and persistent poverty: An
510   asset-based approach. *Journal of Development Studies* **42**, 178–199 (2006).
511   7. A. Kraay, D. McKenzie, Do poverty traps exist? Assessing the evidence. *Journal of*
512   *Economic Perspectives* **28**, 127–48 (2014).
513   8. C. N. Ngonghala, *et al.*, Poverty, disease, and the ecology of complex systems. *PLoS*
514   *Biology* **12**, e1001827 (2014).
515   9. C. N. Ngonghala, *et al.*, General ecological models for human subsistence, health and
516   poverty. *Nature Ecology & Evolution* **1**, 1153–1159 (2017).
517   10. F. J. Zimmerman, M. R. Carter, Asset smoothing, consumption smoothing and the
518   reproduction of inequality under risk and subsistence constraints. *Journal of Development*
519   *Economics* **71**, 233–260 (2003).
520   11. E. B. Barbier, J. P. Hochard, Poverty-environment traps. *Environmental and Resource*
521   *Economics* **74**, 1239-1271 (2019).
522   12. J. R. Rohr, *et al.*, Emerging human infectious diseases and the links to global food
523   production. *Nature Sustainability* **2**, 445–456 (2019).
524   13. J. R. Rohr, *et al.*, A planetary health innovation for disease, food and water challenges in
525   Africa. *Nature* **619**, 782–787 (2023).
526   14. P. Steinmann, J. Keiser, R. Bos, M. Tanner, J. Utzinger, Schistosomiasis and water
527   resources development: Systematic review, meta-analysis, and estimates of people at
528   risk. *The Lancet Infectious Diseases* **6**, 411–425 (2006).
529   15. B. Gryseels, K. Polman, J. Clerinx, L. Kestens, Human schistosomiasis. *The Lancet* **368**,
530   1106–1118 (2006).
531   16. P. J. Hotez, *et al.*, The global burden of disease study 2010: Interpretation and
532   implications for the neglected tropical diseases. *PLoS Neglected Tropical Diseases* **8**,
533   e2865 (2014).
534   17. F. Stelma, I. Talla, P. Verle, M. Niang, B. Gryseels, Morbidity due to heavy Schistosoma
535   mansoni infections in a recently established focus in northern Senegal. *The American*
536   *Journal of Tropical Medicine and Hygiene* **50**, 575–579 (1994).
537   18. C. J. Haggerty, *et al.*, Aquatic macrophytes and macroinvertebrate predators affect
538   densities of snail hosts and local production of schistosome cercariae that cause human
539   schistosomiasis. *PLoS Neglected Tropical Diseases* **14**, e0008417 (2020).
540   19. C. H. King, K. Dickman, D. J. Tisch, Reassessment of the cost of chronic helminthic
541   infection: a meta-analysis of disability-related outcomes in endemic schistosomiasis. *The*
542   *Lancet* **365**, 1561–1569 (2005).
543   20. E. F. Kjetland, *et al.*, Association between genital schistosomiasis and HIV in rural
544   Zimbabwean women. *AIDS* **20**, 593–600 (2006).
545   21. A. Z. Mohammed, S. T. Edino, A. A. Samaila, Surgical pathology of schistosomiasis.
546   *Journal of the National Medical Association* **99**, 570 (2007).
547   22. N. T. Halstead, *et al.*, Agrochemicals increase risk of human schistosomiasis by
548   supporting higher densities of intermediate hosts. *Nature Communications* **9**, 1–10
549   (2018).

23. S. Liang, E. M. Abe, X.-N. Zhou, Integrating ecological approaches to interrupt schistosomiasis transmission: Opportunities and challenges. *Infectious Diseases of Poverty* **7**, 1–6 (2018).

24. J. E. Grimes, *et al.*, The roles of water, sanitation and hygiene in reducing schistosomiasis: A review. *Parasites & Vectors* **8**, 1–16 (2015).

25. C. M. Hoover, *et al.*, Modelled effects of prawn aquaculture on poverty alleviation and schistosomiasis control. *Nature Sustainability* **2**, 611–620 (2019).

26. J. M. Spiegel, *et al.*, Which new approaches to tackling neglected tropical diseases show promise? *PLoS Med.* **18**, e1000255 (2010).

27. J. Utzinger, *et al.*, Schistosomiasis and Neglected Tropical Diseases: Towards Integrated and Sustainable Control and a Word of Caution. *Parasitology* **136**, 1859–74 (2009).

28. S. Gao, Y. Liu, Y. Luo, D. Xie, Control problems of a mathematical model for schistosomiasis transmission dynamics. *Nonlinear Dynamics* **63**, 503–512 (2011).

29. K. L. Bardosh, *et al.*, Addressing vulnerability, building resilience: Community-based adaptation to vector-borne diseases in the context of global change. *Infect Dis Poverty* **6**, 166 (2017).

30. I. Singh, L, Squire, J. Strauss J, *Agricultural Household Models: Extensions, Applications, and Policy*. (John Hopkins University Press Baltimore, 1986).

31. C. B. Barrett, P. Arcese, Wildlife harvest in integrated conservation and development projects: Linking harvest to household demand, agricultural production, and environmental shocks in the Serengeti. *Land Economics* 449–465 (1998).

32. E. C. Stephens, *et al.*, Modeling the impact of natural resource-based poverty traps on food security in Kenya: The Crops, Livestock and Soils in Smallholder Economic Systems (CLASSES) model. *Food Security* **4**, 423–439 (2012).

33. R. Damania, R. Stringer, K. Ullas Karanth, B. Stith, The economics of protecting tiger populations: Linking household behavior to poaching and prey depletion. *Land Economics* **79**, 198-216 (2003).

34. R. Damania, E. J. Milner-Gulland, D. J. Crookes, A bioeconomic analysis of bushmeat hunting. *Proceedings of the Royal Society B: Biological Sciences* **272**, 259-266 (2005).

35. M. Sheahan, C. B. Barrett, C. Goldvale, Human health and pesticide use in sub-Saharan Africa. *Agricultural Economics* **48**, 27-41 (2017).

36. A. Langyintuo, "Smallholder Farmers' Access to Inputs and Finance in Africa" in The Role of Smallholder Farms in Food and Nutrition Security, S. Gomez y Paloma, L. Risego, K. Louhichi, Eds. (Springer Charm, 2020), pp. 133–152.

37. E. B. Barbier, Habitat loss and the risk of disease outbreak, *Journal of Environmental Economics and Management* **108**, 102451 (2021).

38. Mahon *et al.*, A meta-analysis on global change drivers and the risk of infectious disease. *Nature* **628**, 830-836 (2024).

39. K. H. Nguyen, *et al.*, Interventions can shift the thermal optimum for parasitic disease transmission. *Proceedings of the National Academy of Sciences* **118**, e2017537118 (2021).

40. Barbier, E, Valuing ecosystem services as productive inputs. *Economic Policy* **22**, 178-229 (2007).

41. E. Miguel, M. Kremer, Worms: Identifying impacts on education and health in the presence of treatment externalities. *Econometrica* **72**, 159–217 (2004).

42. O. Ozier, Exploiting externalities to estimate the long-term effects of early childhood deworming. *American Economic Journal: Applied Economics* **10**, 235–62 (2018).

43. S. Baird, J. H. Hicks, M. Kremer, E. Miguel, Worms at work: Long-run impacts of a child health investment. *Quarterly Journal of Economics* **131**, 1637-1680 (2016).

44. J. Hamory, E. Miguel, M. Walker, M. Kremer, S. Baird, Twenty-year economic impacts of deworming. *Proceedings of the National Academy of Sciences* **118**, e2023185118 (2021).

45. J. D. Liberatos, *Schistosoma mansoni:* Male-based sex ratios in snails and mice. *Experimental Parasitology* **64**, 165-177 (1987).

46. T. Iverson, E. Barbier, National and Sub-National Social Distancing Reponses to COVID-19. *Economies* **9**, 69 (2021).

47. A. J. Lund, *et al.*, Unavoidable risks: Local perspectives on water contact behavior and implications for schistosomiasis control in an agricultural region of northern Senegal. *American Journal of Tropical Medicine and Hygiene* **101**, 837 (2019).

48. WAEMU Commission, Harmonized Survey on Households Living Standards, Senegal 2018-2019. Ref. SEN_2018_**EHCVM**_v02_M. 2018; Dataset downloaded from www.microdata.worldbank.org on September 23, 2022.

49. M. Schiavina, S. Freire, A. Carioli, K. MacManus, GHS-POP R2023A – GHS population grid multitemporal (1975-2030), European Commission, Joint Research Centre (JRC). 2023; Dataset downloaded from 10.2905/2FF68A52-5B5B-4A22-8F40-C41DA8332CFE on June 21, 2024.
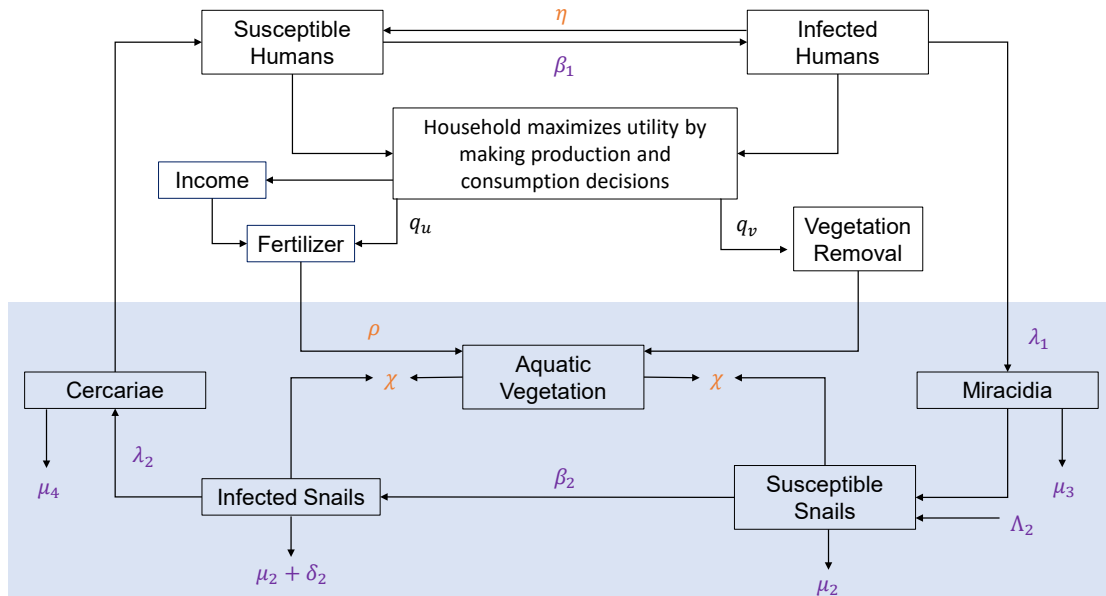
50. Food and Agriculture Organization of the United Nations (FAO). Rivers of Africa AQUASTAT. 2022; Dataset downloaded from data.apps.fao.org on June 21, 2024.

51. M. L. Messager, B. Lehner, G. Grill, I. Nedeva, O. Schmitt. Estimating the volume and age of water store in global lakes using a geo-statistical approach. *Nature Communications* **7**, 13603 (2016).

14

Figures and Tables

Figure 1. Flow chart describing the relationship between model populations and parameters. This flow chart describes how the key populations of the economic and disease-ecology submodels (in boxes) interact with each other. Arrows represent links between populations and these links are governed by the parameters next to the arrows. The blue shaded area represents water. Arrows in and out without boxes represent births and deaths within the model. All parameters in orange were added to the model developed by Gao and colleagues.[28] The parameters in black are results of household's optimization problem. This figure was adapted from Nguyen and colleagues.[39]

634
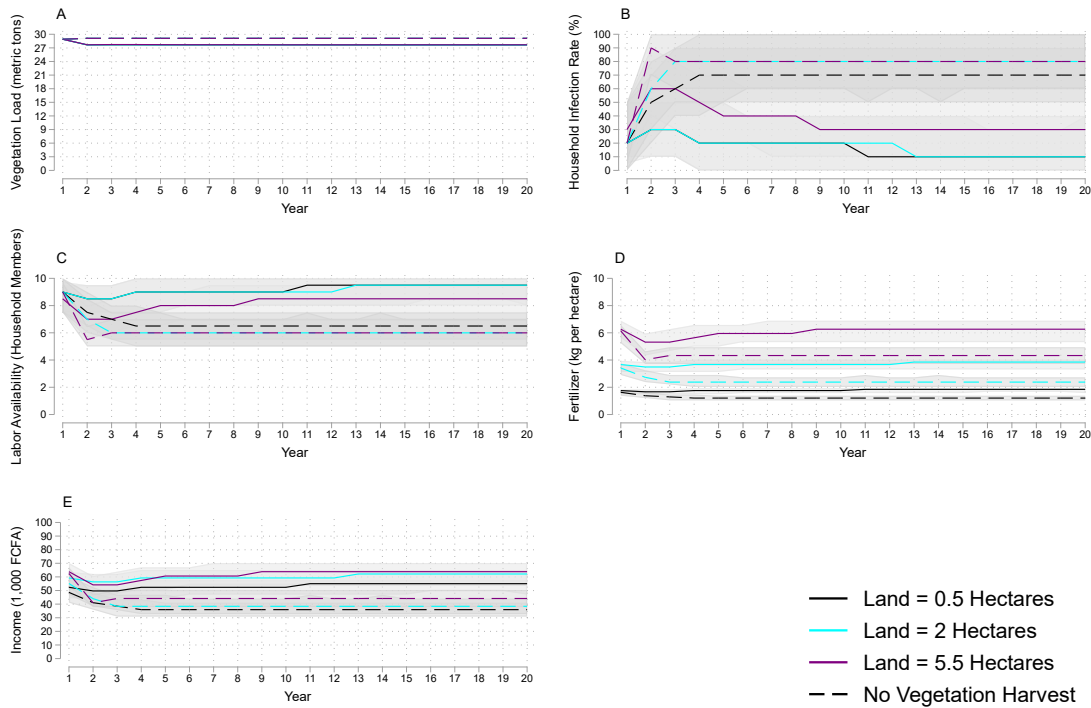
635
636 **Figure 2. Median vegetation load, infection rate, labor availability, fertilizer use, and**
637 **income for simulations with and without vegetation harvest.** Panel A plots the median
638 aquatic vegetation stock (population) in metric tons across 1,000 20-year simulations for three
639 different household land endowments with (solid lines) and without (dashed lines) vegetation
640 harvest. Aquatic vegetation load represents the size of the snail habitat within the village water
641 access point used by the household. Shaded areas represent the 5-95 percent centered
642 confidence band. Based on scale and precision, not all shaded areas are visible. Panel B shows
643 the median household infection rate (the number of infected individuals divided by total number of
644 household members). Panel C reports median labor availability from the 10-person household
645 size maximum. Panel D displays median fertilizer use in kgs per hectare, and Panel E reports the
646 median income in FCFA1,000. Medians and percentiles are within each land endowment each
647 time period across the 1,000 simulations.
648
649

650
651 **Figure 3. Median first year optimal fertilizer use at different infection levels.** Figure 2 plots
652 median fertilizer use in kgs per hectare in the first year across 1,000 20-year simulations for the
653 median household land endowments with vegetation harvest. Shaded areas represent the 5-95
654 percent centered confidence band. Only the initial starting infection probability was modified. All
655 other disease ecology submodel parameters remain the same.
656
657
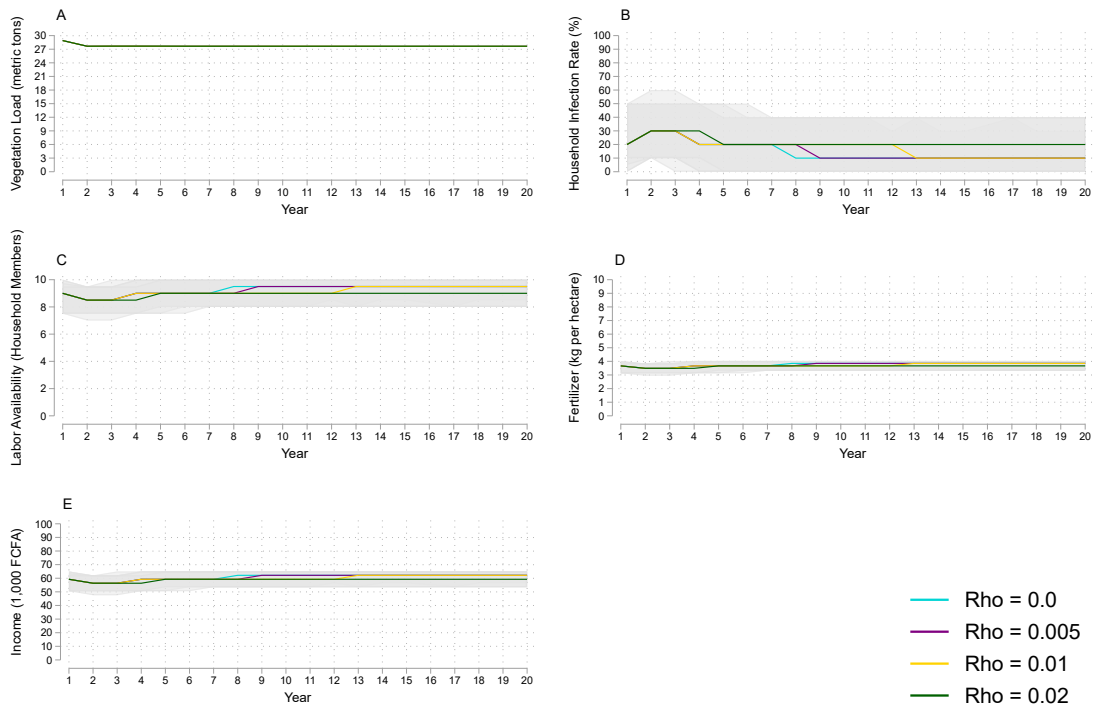
658
659 **Figure 4. Median vegetation load, infection rate, labor availability, fertilizer use, and**
660 **income for the fertilizer effect sensitivity analysis.** Panel A plots the median aquatic
661 vegetation stock (population) in metric tons across 1,000 20-year simulations for four different
662 levels of feedback between fertilizer runoff and vegetation growth (ρ) and households with two
663 hectares of land. Aquatic vegetation load represents the size of the snail habitat within the village
664 water access point used by the household. Shaded areas represent the 5-95 percent centered
665 confidence band. Based on scale and precision, not all shaded areas are visible. Panel B shows
666 the median household infection rate (the number of infected individuals divided by total number of
667 household members). Panel C reports median labor availability from the 10-person household
668 size maximum. Panel D displays median fertilizer use in kgs per hectare, and Panel E reports the
669 median income in FCFA1,000. Medians and percentiles are within each land endowment each
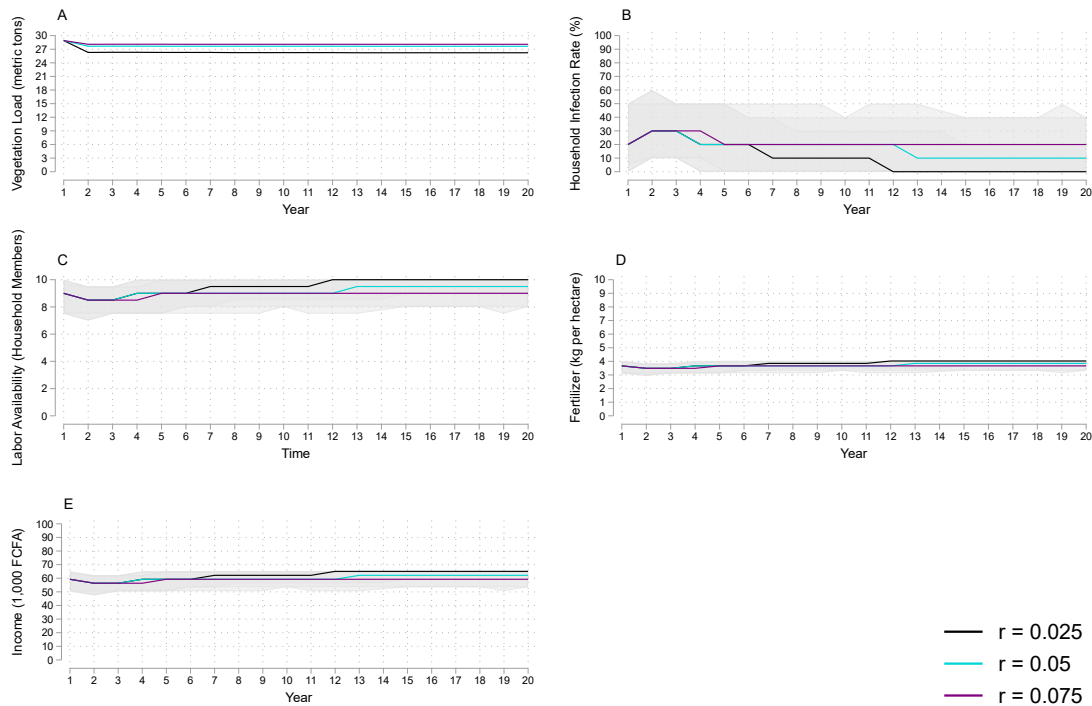670 time period across the 1,000 simulations.
671
672

Figure 5. Median vegetation load, infection rate, labor availability, fertilizer use, and income for the vegetation growth rate sensitivity analysis. Panel A plots the median aquatic vegetation stock (population) in metric tons across 1,000 20-year simulations for three different levels of the vegetation growth rate (r) and households with two hectares of land. Aquatic vegetation load represents the size of the snail habitat within the village water access point used by the household. Shaded areas represent the 5-95 percent centered confidence band. Based on scale and precision, not all shaded areas are visible. Panel B shows the median household infection rate (the number of infected individuals divided by total number of household members). Panel C reports median labor availability from the 10-person household size maximum. Panel D displays median fertilizer use in kgs per hectare, and Panel E reports the median income in FCFA1,000. Medians and percentiles are within each land endowment each time period across the 1,000 simulations.

Supplementary Materials

SI Appendix Text S1. More Information on the Literature and Context of the Study

Poverty-Disease Traps
Poverty-disease traps, perhaps first mathematically modeled by Bonds and colleagues,[1] connect a classic susceptible-infected-susceptible (SIS) general disease model to income where key model parameters that define death, recovery, transmission, and general infection are functions of income, and income is a function of infection. This reduced form empirical model, and expansions on it, [2-8] fall into two broad categories, those that maintain the basic feedback loop Bonds and colleagues employ[1] but add stochasticity or other refinements[7] and those that apply the idea of a poverty-disease trap to other modeling frameworks.[2,4-6,8]

The primary extension of the basic model in the literature comes from connecting a neoclassical macroeconomic growth model to a disease ecology model where capital accumulation depends on infection.[5,8] The systems exhibit evidence of multiple equilibrium poverty traps.[5,8] Such models lack a micro-economic foundation to explain individuals' decisions, however, which makes it somewhat difficult to understand the structural behavioral foundations of the reduced form relationships that underpin the model. Ngonghala and colleagues[6] develop 11 different versions of the basic neoclassical growth model that include up to three types of capital (human, physical, and biological) and populations of natural enemies, parasites, pests, and predators. Goenka and Liu[4] add public or private investment to control disease transmission to the macro-level neoclassical growth model. The authors find disease slows growth and makes poverty traps possible. These neoclassical growth models consider only larger aggregates of people: villages or countries.

A much smaller literature looks at individual or household decision making relating to malaria in Uganda[2] and Buruli ulcer.[3] Berthélemy and colleagues[2] use theoretical models to derive the infectiousness of malaria and then demonstrate under which conditions the spread of malaria might result in a poverty trap. Garchitorena and colleagues[3] model the individual or household with a Cobb-Douglas production function and they find that even with relatively low incidence of disease, as with Buruli ulcer, poverty-disease traps are possible, especially when areas start with high levels of poverty. However, these economic models do not include clear modelling of the tradeoffs faced by individuals making decisions. The authors instead model the decision to treat a disease with random draws based on exogenous probability distributions.

This paper uses the analytical base of the microeconomic behavior of a household that makes optimal decisions and faces trade-offs because of binding budget and time constraints. By explicitly depicting the primal structural problem that households face when making choices subject to constraints, we demonstrate not only *that* households can be trapped in poverty due to infectious disease exposure, but also can identify *why* and thus *how* one might change underlying behaviors and outcomes. Indeed, this framework allows us to consider the formal comparative statistics of the household's constrained optimization problem, to explore how changes in prices or quantities of goods impact the household's optimal decisions, in addition to simulate the system empirically to allow us to better identify feedback loops within the system and thus how and why a specific intervention works – or fails to work – to reduce infection and poverty rates.

Senegalese Context
The geographical context for this paper is the Senegal River Valley and the Saint Louis and Louga regions in northern Senegal. The 1988 construction of the Diama dam, near the mouth of the Senegal River, dramatically changed land use in the region, particularly along the shores of the Senegal River and Lac de Gueirs, the largest basin within the region.[9,10] The creation of irrigation canals and the subsequent desalination of the water expanded the habitat of *Bulinus* and *Biomphalaria* snails, the intermediate vectors for schistosomiasis transmission. *S. mansoni* and *S. haematobium* are currently endemic within the region.[10] About 75% of school children within 16 study villages in the region were infected with *S. haematobium*, a urogenital

schistosomiasis infection, while 25% of school children were infected with *S. mansoni*, a colorectal infection; many of the children infected with *S. mansoni* are also infected with *S. haematobium*.[11] Around 90% of cattle within the region were infected with *Schistosomiasis bovis* (a livestock variant of schistosomiasis), and many of the *S. haematobium* infections within humans in the region are *S. haematobium - S. bovis* hybrid infections.[10]

Villages within the region are small, typically with populations between 1,000 and 5,000 residents.[11] Households within this region are largely agricultural, predominately growing rice, millet, cowpea, and peanuts.[12] Other horticulture crops are commonly grown in smaller plots. Many households within these villages rely on surface water sources to wash clothes and dishes, bathe, and irrigate plots. There also is sugar cane production along the northern edge of Lac de Gueirs which contributes to significant fertilizer runoff and ecological concerns, particularly eutrophication, within the lake. Increased nutrient loading within the water source contributes to the growth of *Ceratophyllum demersum*, the aquatic vegetation that is the preferred habitat for snails, and thereby to increased schistosomiasis infection. [13, 14]

The 2018-2019 Harmonized Survey on Household Living Standards in Senegal collected by the West African Economic and Monetary Union (WAEMU) Commission[12],* reports that 30% of the household heads in the survey are female, and on average household size is large with over 10 members per household (table S2). The average household head is 52 years old and over 85% of household heads are married. Literacy rates are low as just under a third of household heads can read and write in French. Just under 30% of households engage in rice cultivation, around 40% of households have irrigation on at least one of their plots, and 45% of households use fertilizer on at least one of their plots. Households devote just under 400 person days to working on their farm across all family members. Just over 40% of households hire outside labor to work on their farm and the average family hires outside labor for 23 person days. Conditional on households hiring any outside labor, households hire on average outside labor for almost 35 person days.

Aquatic Vegetation Removal
Transmission of schistosomiasis occurs through the intermediate vector of aquatic snails. The parasite enters the water source when an infected human or animal (especially, cattle) urinates or defecates in the water releasing schistosome eggs. Once in the water, the eggs release miracidia, the first parasitic larval stage that infects the aquatic snails. After four to six weeks in an infected snail, cercariae, a subsequent larval stage of the parasite, exit the snail. Humans become infected with *Schistosoma* spp. worms through water contact with cercariae that enter the body through the skin.[15]

The aquatic vegetation removal intervention modeled in this paper specifically looks to disrupt the infection cycle through reduced snail habitat. *Bulinus* and *Biomphalaria* snails live in the submergent vegetation, *Ceratophyllum demersum*, in the lakes and rivers of the region. This aquatic vegetation has a symbiotic relationship with the snail population and cercariae.[16] By removing the aquatic vegetation, snails lose their habitat and source of food reducing both the number of snails and the cercariae they release.

Previous experimental work in this region suggests that removing aquatic vegetation from freshwater sources can significantly reduce *S. mansoni* infection in children through decreased snail populations.[11] As such, the bioeconomic model presented in this paper focuses on *S. mansoni* gastrointestinal infection.

Recent crop trials suggest that compost made from harvested vegetation increases onion and pepper yields offering a good substitute for fertilizer.[11] By producing compost from aquatic

vegetation sourced from the system, nitrogen applied on the fields in the form of compost from this vegetation simply recycles nitrogen that already existed within the system. Vegetation removal thus has the possibility to close nitrogen loops within the region, both boosting agricultural productivity by reusing leached nutrients and reducing infection prevalence by reducing snail habitat.

SI Appendix Text S2. Additional Details of the Bioeconomic Model

The Household's Problem
Let i denote each of the different goods a household consumes, produces, or uses as a production input. Let q_i denote the quantity of goods produced or used as production inputs by the household. The household produces ($q_i \geq 0$) of food ($i = f$) using land ($i = d$), labor ($i = l_f$), fertilizer ($i = u$), and compost (ωq_v). The household makes compost from harvested vegetation ($i = v$) and harvesting vegetation requires labor ($i = l_v$). Composting reduces the mass of harvested vegetation, so the fraction of harvested vegetation remaining as compost to use in food production is $\omega \in (0,1)$. Let $L_f = q_{l_f} + L_f^h$ be the total amount of labor used in the production of food and $L_v = q_{l_v} + L_v^h$ be the total amount of labor used to harvest vegetation. The household's production technology for food is then given by $F(L_f, q_d, q_u, \omega q_v)$ and the production technology for harvesting vegetation is $G(L_v)$.

Let c denote the vector of all consumption goods comprised of food ($i = f$), non-food household goods and services ($i = g$), and leisure ($i = l$). Let $H(I_1, S_1, c_f)$ denote the household's health status, which is an decreasing function of I_1, the number of infected individuals in the household, and S_1, the number of not infected (susceptible) individuals in the household,[†] and increasing in c_f, food consumption. We denote household utility as $U(c, H)$.

Each household has endowments of labor e_l and land e_d in each time period. Each household member has one unit of labor; however, infection reduces the labor availability of an individual to τ where $0 \leq \tau < 1$. Infection reduces nutrient absorption from food and results in less labor productivity overall, effectively reducing the labor availability of infected individuals. The labor available to the household a_l is the sum of all household members' labor availability.

A household generates income by growing food. There are perfectly competitive markets for food, the aggregate household good and urea fertilizer (the tradables set $T = \{f, g, l, u\}$), but there are not markets for vegetation, land or health (the non-tradables set $NT = \{d, v, H\}$). Each household must fully self-provide non-tradable goods. Finally, let p_i denote the market price for good i.

Thus, in each period, the household solves the problem:
$$\max_{(c,q)} U(c, H) \tag{1}$$
subject to the cash budget constraint for tradable goods,
$$p_f c_f + p_g c_g \leq p_f \left(F(L_f, q_d, q_u, \omega q_v) \right) \tag{2}$$
the availability constraint for vegetation use,
$$q_v - \beta_v (L_v)^{\gamma 1} \geq 0 \tag{3}$$
the availability constraint for land use,
$$q_d - e_d \geq 0 \tag{4}$$
the time constraint on the household's labor availability,
$$a_l \geq q_{l_f} + q_{l_v} + c_l \tag{5}$$
and the health production function.
$$H = H(I_1, S_1, c_f) \tag{6}$$
We substitute the availability constraint into the food production function in the cash budget constraint and then substitute the labor constraint into the budget constraint to create the full income constraint:

[†] We follow Gao and colleagues'[17] notation for infected (I_1) and susceptible individuals (S_1). We use similar notation for infected and susceptible snails (I_2 and S_2), with the subscript 1 for humans and the subscript 2 for snails.

$$p_f c_f + p_g c_g + w \left(c_l + q_{l_f} + q_{l_v} \right)$$

$$\leq p_f \left(F \left(q_{l_f}, L_f^h, q_d, q_u, \omega q_v \left(q_{l_v}, L_v^h \right) \right) \right) - p_u q_u + w a_l \qquad (7)$$

Requiring all land to be used in production, assuming an interior solution, substituting (6) into (1) and using Lagrange multiplier λ on the household's full income constraint, the first order conditions for the maximization problem are:

$$\frac{\partial U}{\partial c_f} + \frac{\partial U}{\partial H} \frac{\partial H}{\partial c_f} = \lambda p_f \qquad (8)$$

$$\frac{\partial U}{\partial c_g} = \lambda p_g \qquad (9)$$

$$\frac{\partial U}{\partial c_l} = \lambda w \qquad (10)$$

$$p_f \frac{\partial F}{\partial q_{l_f}} = w \qquad (11)$$

$$p_f \frac{\partial F}{\partial q_v} \frac{\partial q_v}{\partial q_{l_v}} = w \qquad (12)$$

$$p_f \frac{\partial F}{\partial q_u} = p_u \qquad (13)$$

Equations (8), (9), and (10) can be rearranged to show that the ratio of the marginal benefit of consuming food (which includes direct increases in utility and indirect utility increases through improved health) to the marginal benefit of consuming the aggregate household good or leisure equals the price ratio. Equations (11) – (13) are input use constraints that require the use of family labor and fertilizer until the value of the marginal product of labor or fertilizer equals its respective cost or opportunity cost in the case of family labor.

Specifically, assume that the household has Cobb-Douglas utility:

$$U(\boldsymbol{c}, H) = c_f^{\theta_f} c_g^{\theta_g} H^{\theta_h} c_l^{\theta_l} \qquad (14)$$

where the θ's add up to one. We calibrate the parameters $\boldsymbol{\theta}$ by estimating expenditure shares from the Harmonized Survey on Household Living Standards 2018-2019 in Senegal.[12] Expenditure shares can be found in table S3. We set $\theta_f = 0.5$, $\theta_g = 0.3$, $\theta_h = 0.1$, and $\theta_l = 0.05$.

Health status follows the health production function given by

$$H = \exp\left(\frac{S_1}{I_1 + S_1}\right) c_f^{h_f} \qquad (15)$$

where I_1 is infected household members, S_1 is not infected household members, and h_f is the elasticity of the increase in health from food consumption and we set $h_f = 0.000384$.[18,19] Production of food takes the CES form:

$$q_f = \left(\alpha_d q_d^\phi + \alpha_l \left(q_{l_f} + L_f^h \right)^\phi + \alpha_u q_u^\phi + \alpha_v (\omega q_v)^\phi \right)^{1/\phi} \qquad (16)$$

We estimate factor cost shares from the Harmonized Survey on Household Living Standards 2018-2019 in Senegal to determine the parameters α_d, α_l, α_u, and α_v and calibrate ϕ to achieve fertilizer use consistent with observed patterns.[12] Estimated factor cost shares can be found in table S4. We set $\alpha_d = 0.4$, $\alpha_l = 0.5$, $\alpha_u = 0.05$, $\alpha_v = 0.05$, and $\phi = 0.3$. We consider labor shares in the model. We scale the production function to labor days based on the average amount of labor allocated to a plot within the survey data as the unit of labor is important for understanding the returns to labor.[20]

We model vegetation harvest as

$$q_v = \beta_v \left(q_{l_v} + L_v^h\right)^{\gamma 1} \tag{17}$$

where we set $\beta_v = 14.4942$ and $\gamma 1 = 0.2595$ using estimates of harvested vegetation and labor data from Rohr and colleagues.[11,‡] We set the price of food, $p_f = 290$ FCFA to the average, location-adjusted price of local rice estimated from Senegalese price reports.[21] We calibrate the price of fertilizer to be consistent with household survey data[12] and to achieve stable aquatic vegetation populations. We set $p_u = 300$ FCFA. We set the price of the aggregate household good to $p_g = 500$ FCFA. In the simulations, we normalize all prices setting the price of food equal to one. A summary of the parameter values used in the household model is presented in table S5.

With these parameters and prices, we can calculate the ratio of the estimated marginal revenue product of fertilizer relative to the prices of fertilizer at the sample means of land, food labor, and vegetation labor provided by the household in these simulations. We calculate this ratio over the observed rates of fertilizer application rates within our simulation and for different fertilizer prices. At the baseline price of fertilizer, this ratio is over 4 and it drops to 2 for the highest price fertilizer simulation in the sensitivity analysis. Thus, fertilizer use is limited by the budget constraint within our simulations for this context.

Disease Ecology Model for Schistosomiasis
Ceratophyllum is the keystone aquatic vegetation species in this system. Its population follows a logistic growth function. The population also depends on the amount of vegetation removed by household members or hired workers q_v. With a starting density of N_0, the population density of aquatic vegetation is

$$\frac{dN}{dt} = r \times N \times \left(1 - \frac{N}{K}\right) + n0 - \frac{q_{v_t}}{365} \tag{18}$$

where r is the net growth rate of *Ceratophyllum*, K is the carrying capacity of the freshwater environment, $n0$ is the recruitment rate of new aquatic vegetation from other parts of the lake or river, and q_{v_t} is the amount of harvested aquatic vegetation, i.e., the household's production of harvested vegetation which is then divided by 365 to model small amounts of daily vegetation harvest by the household. Households harvest vegetation daily as they continuously update their labor allocations consistent with Fafchamps[22] and Dillon[23]. The amount of aquatic vegetation to start each period is $N_{t+1} = N_t + \rho \times q_{u_t} \times N_t$ where $\rho \times q_{u_t} \times N_t$ captures the impact of urea fertilizer use, q_{u_t}, on vegetation growth as Rohr and colleagues[11,13] reports that agrochemicals like fertilizer contribute to vegetation growth. We estimate the carrying capacity and starting value of *Ceratophyllum* based on the average amount of vegetation found within water access points sampled by Rohr and colleagues,[11] setting $K = 28,906.5\ kg$ and $N_0 = 28,906.5\ kg$. We set $r = 0.05$, $\rho = 0.01$, and $n0 = 0.01$. Table S6 summarizes all parameters in the disease ecology model.

Aquatic vegetation affects the snail population, both susceptible and infected, which we model by

$$\frac{dS_2}{dt} = \Lambda_2 - \frac{\beta_2 M S_2}{M_0 + \epsilon M^2} - \left(\mu_2 + \chi(K - N)\right)S_2 \tag{19}$$

$$\frac{dI_2}{dt} = \frac{\beta_2 M S_2}{M_0 + \epsilon M^2} - \left(\mu_2 + \delta_2 + \chi(K - N)\right)I_2 \tag{20}$$

where Λ_2 is the recruitment rate of susceptible snails, β_2 is the probability of snail infection from miracidia, M_0 is the contact rate between miracidia and snails, ϵ is the saturation coefficient for miracidial infectivity, μ_2 is the natural death rate of snails, δ_2 is the death rate of snails from infection, and χ is the death rate of snails from a one kg decrease in vegetation. We set $M_0 = 1.0 \times 10^6$, $\epsilon = 0.3$, $\Lambda_2 = 100$, $\beta_2 = 0.615$, $\mu_2 = 0.008$, and $\delta_2 = 0.0004012$,[17] while we estimate $\chi = 0.02842$ from aquatic vegetation removal data.[11,§]

---

‡ Details of the estimation can be found in SI Appendix Text S3 and results are in table S8.
§ We estimate χ using a simple calculation comparing the average mass of aquatic vegetation removed at each site to the average drop in snail population after removal.

The miracidia population follows

$$\frac{dM}{dt} = k\lambda_1 I_1 - \mu_3 M \tag{21}$$

where k is the number of eggs released into the environment per human host, λ_1 is the hatching rate for miracidia, and μ_3 is the miracidial mortality rate. We set $k = 300$, $\lambda_1 = 50$, and $\mu_3 = 2.5$.[17,24] The cercariae population follows

$$\frac{dP}{dt} = \lambda_2 I_2 - \mu_4 P \tag{22}$$

where λ_2 is the cercarial emergence rate and μ_4 is the cercarial mortality rate. We assume there is no cercarial elimination intervention. We estimate the model with $\lambda_2 = 2.6$ and $\mu_4 = 0.004$.[17]

Finally, the susceptible and infected human populations follow

$$\frac{dS_1}{dt} = -\frac{\beta_1 P S_1}{1 + \alpha_1 P} + \eta I_1 \tag{23}$$

$$\frac{dI_1}{dt} = \frac{\beta_1 P S_1}{1 + \alpha_1 P} - \eta I_1 \tag{24}$$

Where β_1 is the contact between cercariae and humans, α_1 is the saturation coefficient for cercarial infectivity, and η is the treatment rate of infected humans. We assume that schistosomiasis infections cause neither birth nor deaths of humans. The unconditional mortality rate of humans due to schistosomiasis is around $\frac{1}{1,000}$.[25] Since we consider villages with average populations around 5,000 with infections around $1,000 - 4,000$ at any given time, deaths from schistosomiasis are relatively rare. Thus, we abstract away from the disease's mortality effects and instead focus only on the morbidity impacts through reduced labor productivity. Because we only consider relatively short time periods, we treat the household population as stable and focus on labor availability dynamics within the household. We set $\beta_1 = 1.766 \times 10^{-8}$ and $\alpha_1 = 0.8 \times 10^{-8}$.[17] We set $\eta = 0.0068$ to model some infected individuals receiving treatment through deworming medications (e.g., praziquantel) during sporadic mass deworming events. However, it is expensive to diagnose schistosomiasis and treatment of infections remains relatively infrequent even with mass deworming events that often do not diagnose individuals before they receive deworming medication.

Initial population sizes for all relevant populations in the disease ecology submodel are reported in table S7.

SI Appendix Text S3. Additional Information on Estimating Aquatic Vegetation Harvest

We use experimental field trial data collected from Rohr and colleagues[26] on the amount of vegetation removed and the number of labor days devoted to harvesting vegetation to estimate the parameters in the production function of harvested vegetation (Equation 17). We estimate the harvested vegetation production as

$$\ln(Kg\ of\ harvested\ vegetation)_i = \alpha + \beta \ln(person\ days)_i + \varepsilon_i \tag{25}$$

The coefficient estimate β is our direct estimate of $\gamma 1$ in Equation 19 and we calculate β_v from the estimate of the constant α using $\beta_v = \exp(\alpha)$. Results from the estimation are reported in table S8.

SI Appendix Text S4. Additional Details on Disease Ecology Submodel Parameterization

We base the disease ecology submodel on Gao and colleagues.[17] We use experimental estimates of parameters in the local population in Senegal from Nguyen and colleagues[24] as a guide to adjust model parameters to match human infection levels observed within the region. Table S7 reports and describes the starting parameters we used to simulate the model. We excluded human births and deaths from this simulation.[**]

The continuous time equations are:
Susceptible snails:

$$\frac{dS_2}{dt} = \Lambda_2 - \frac{\beta_2 M S_2}{M_0 + \epsilon M^2} - \mu_2 S_2 \tag{26}$$

Infected snails:

$$\frac{dI_2}{dt} = \frac{\beta_2 M S_2}{M_0 + \epsilon M^2} - (\mu_2 + \delta_2) I_2 \tag{27}$$

Cercariae:

$$\frac{dP}{dt} = \lambda_2 I_2 - \mu_4 P \tag{28}$$

Susceptible Humans:

$$\frac{dS_1}{dt} = -\frac{\beta_1 P S_1}{1 + \alpha_1 P} + \eta I_1 \tag{29}$$

Infected Humans:

$$\frac{dI_1}{dt} = \frac{\beta_1 P S_1}{1 + \alpha_1 P} - \eta I_1 \tag{30}$$

Miracidia:

$$\frac{dM}{dt} = k \lambda_1 I_1 - \mu_3 M \tag{31}$$

Modifications
We calibrated the human population to match the household-level analysis in the Senegalese context. The household size is set at 10 where 7.5 humans start as susceptible and 2.5 are infected, matching the 25% baseline prevalence of *S. mansoni* in the region reported by Rohr and colleagues.[11,††] Modifications to the original model parameters reported in Gao and colleagues[17] are required because we significantly reduce the size of the human population and eliminate human births and deaths to integrate the disease ecology model of schistosomiasis with an economic model of agricultural households.

We start with the parameters in Gao and colleagues,[17] reported in table S9, and then calibrate the model from these parameter starting points with the goal of finding a steady state at or very close to 25% infection with 10 humans in the model (so 7.5 susceptible humans and 2.5 infected humans). We calibrate the parameters to achieve population stability in the snails and then increase infection until the human infection stabilized near 25%.

Finally, we added vegetation into the model. We use a general logistic growth function for vegetation, where r is the growth rate, K is the carrying capacity, and $n0$ is the natural recolonization rate. The carrying capacity was estimated from vegetation data.[11] We chose the

---

[**] Over a relatively short time horizon, 20 years or less, assuming away human population growth or decline for an individual family is reasonable as it represents roughly one generation.
[††] Note, we cannot have 7.5 infected and 2.5 susceptible humans in the numerical simulations. We start the model at these values to match the 25% infection rate reported by Rohr and colleges.[11] The first period (and all period) simulation draws are integers for infected and susceptible humans. The non-integer values only occur in the initial state to start the simulation process.

growth rate and the recolonization rate to match rapid regrowth consistent with rates observed at study sites in Rohr and colleagues.[11] The logistic growth function is reported below:

$$\frac{dN}{dt} = r \times N \times \left(1 - \frac{N}{K}\right) + n0 \tag{32}$$

To connect vegetation to the existing system, a parameter χ is added to the snails' population equations. For every kilogram of vegetation below the carrying capacity, the snail population is reduced by χ percent. We start the vegetation population at the carrying capacity and do not include vegetation removal and thus vegetation has no effect on the other populations in these model runs. Table S10 reports all starting values and adjusted parameters.

Simulations
Results from the simulations for each of key populations can be found in figure S4. We present five-year models of simulations without vegetation to confirm we have found a steady state within the disease ecology submodel. Since the vegetation population is started at the steady state level, it does not affect how the rest of the model operates and thus is not needed in these extra simulations to confirm the snails, humans, miracidia, and cercariae populations approach a steady state.

Supplemental Figures

Figure S1. Median vegetation load, infection rate, labor availability, fertilizer use, and income for the recolonization rate sensitivity analysis. Panel A (top left) plots the median aquatic vegetation stock (population) in metric tons across 1,000 20-year simulations for three different levels of the vegetation recolonization rate ($n0$) and households with two hectares of land. Aquatic vegetation load represents the size of the snail habitat within the village water access point used by the household. Shaded areas represent the 5-95 percent centered confidence band. Based on scale and precision, not all shaded areas are visible. Panel B shows the median household infection rate (the number of infected individuals divided by total number of household members). Panel C reports median labor availability from the 10-person household size maximum. Panel D displays median fertilizer use in kgs per hectare, and Panel E reports the median income in FCFA1,000. Medians and percentiles are within each land endowment each time period across the 1,000 simulations.
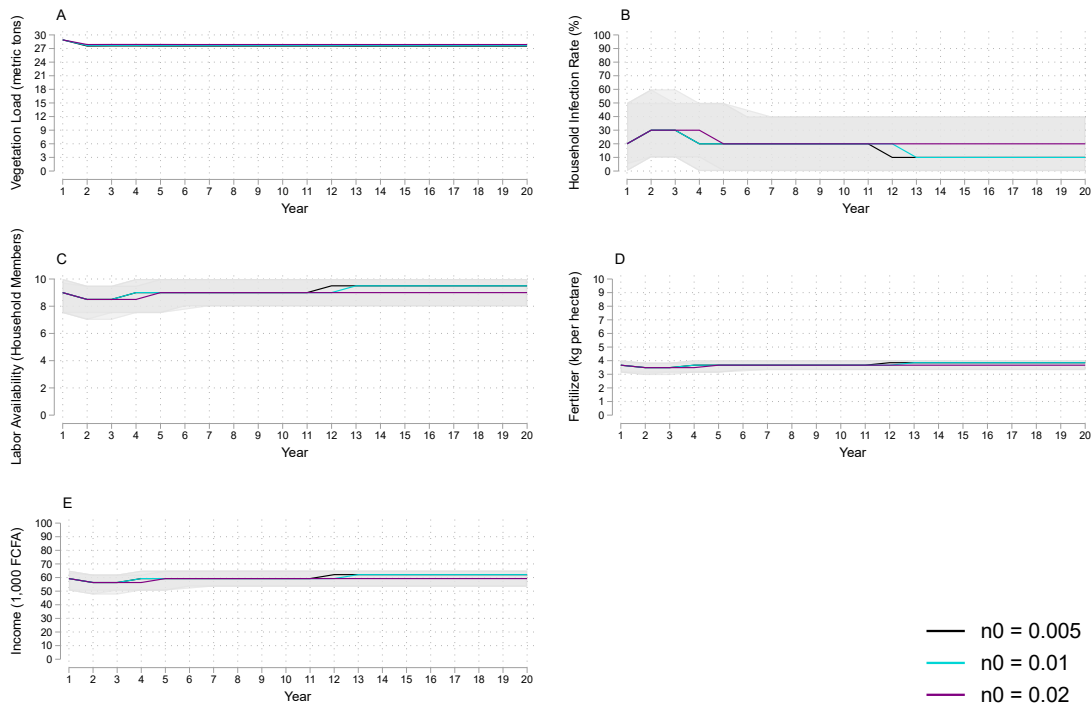
Figure S2. Median vegetation load, infection rate, labor availability, fertilizer use, and income for the fertilizer price sensitivity analysis. Panel A (top left) plots the median aquatic vegetation stock (population) in metric tons across 1,000 20-year simulations for three different levels of fertilizer prices (p_u) and households with two hectares of land. Aquatic vegetation load represents the size of the snail habitat within the village water access point used by the household. Shaded areas represent the 5-95 percent centered confidence band. Based on scale and precision, not all shaded areas are visible. Panel B shows the median household infection rate (the number of infected individuals divided by total number of household members). Panel C reports median labor availability from the 10-person household size maximum. Panel D displays median fertilizer use in kgs per hectare, and Panel E reports the median income in FCFA1,000. Medians and percentiles are within each land endowment each time period across the 1,000 simulations.

Figure S3. Median vegetation load, infection rate, labor availability, fertilizer use, and income for the household good price sensitivity analysis. Panel A (top left) plots the median aquatic vegetation stock (population) in metric tons across 1,000 20-year simulations for three different levels of household good prices (p_h) and households with two hectares of land. Aquatic vegetation load represents the size of the snail habitat within the village water access point used by the household. Shaded areas represent the 5-95 percent centered confidence band. Based on scale and precision, not all shaded areas are visible. Panel B shows the median household infection rate (the number of infected individuals divided by total number of household members). Panel C reports median labor availability from the 10-person household size maximum. Panel D displays median fertilizer use in kgs per hectare, and Panel E reports the median income in FCFA1,000. Medians and percentiles are within each land endowment each time period across the 1,000 simulations.
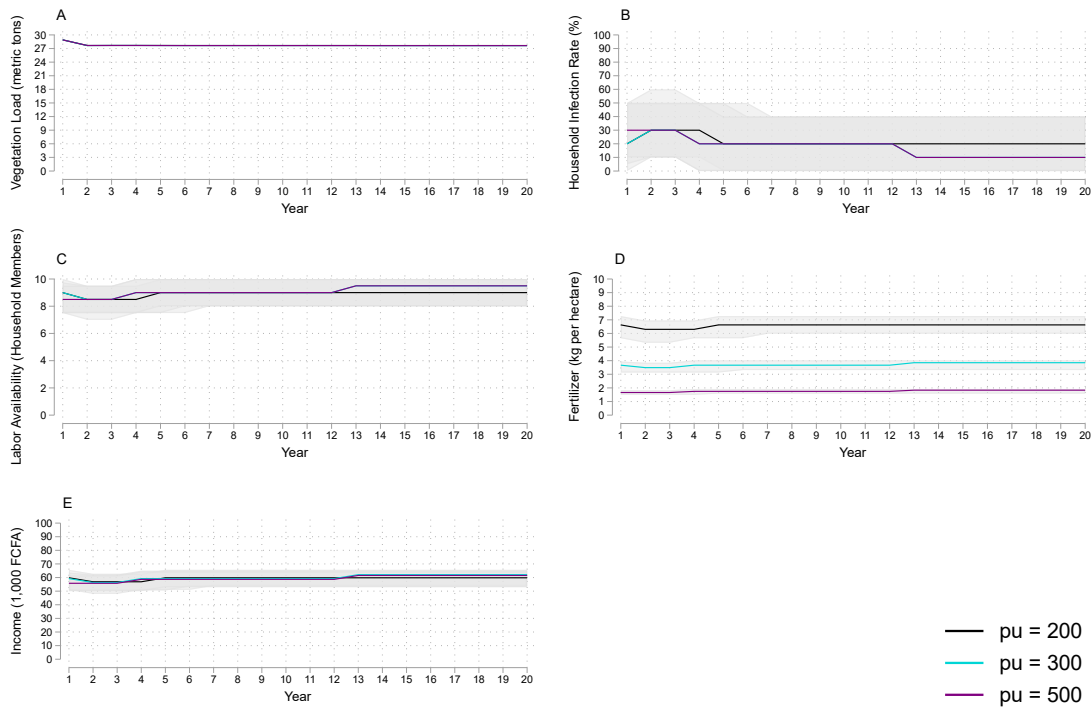
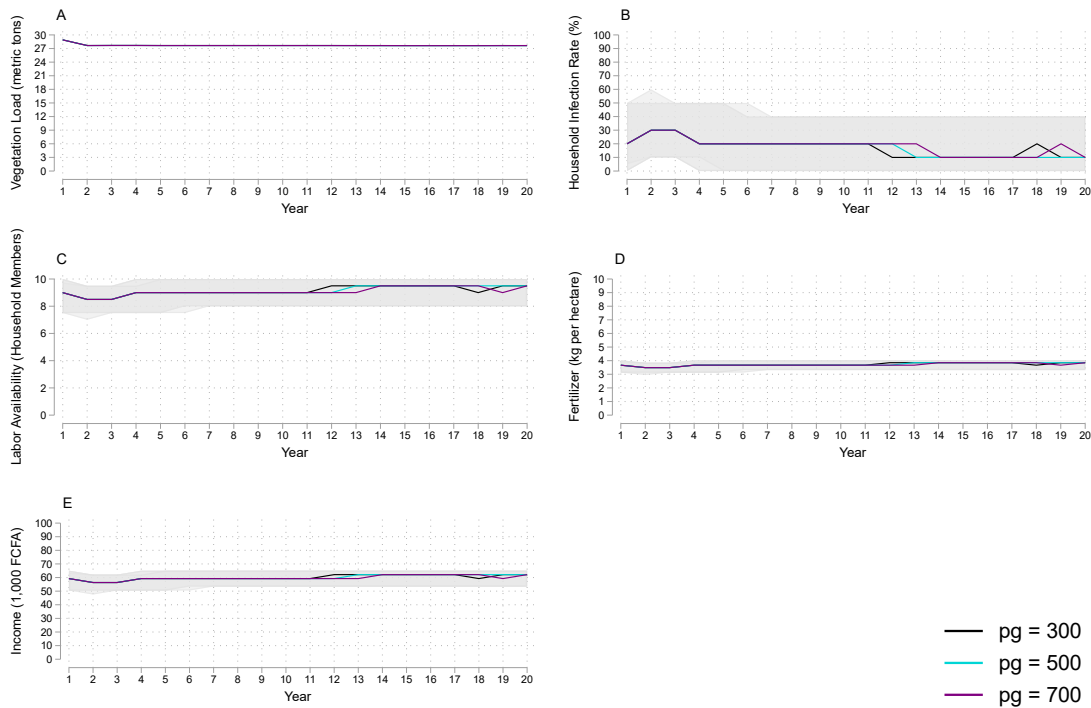**Figure S4. Five-year continuous time simulation results.** Simulation results are for the modified disease ecology model. Vegetation is omitted as it is set to the carrying capacity and has no effect on the system in this stable state.

Supplemental Tables

Table S1. Land endowments for household simulations. Land holdings based on the 25th, 50th, and 75th percentiles in the Saint Louis and Louga regions from the Harmonized Survey on Household Living Standards in Senegal collected in 2018 and 2019.

Type	Land Endowment (hectares)
25th percentile	0.5
50th percentile	2
75th percentile	5.5

Table S2. Summary statistics of agricultural households in the Saint Louis and Louga regions. Summary statistics for households in the Saint Louis and Louga regions of the 2018-2019 Harmonized Survey on Household Living Standards in Senegal. Household size is calculated by summing the number of household members included in the member module of the survey. Household farm labor and outside labor includes labor of all household members across the following tasks: preparing the plot, weeding, and harvesting. Female indicates that the household head is female. Read French and Write French indicate that the household head can read or write in French, respectively. Formal school indicates that the household head attended formal schooling. Hire outside labor indicates that the household hired at least one person day of labor from an individual outside the family. Rice, Millet, Cowpea, and Peanut indicates that the household in engaged in rice, millet, cowpea, or peanut cultivation, respectively. Irrigation and Fertilizer indicate that at least one household plot is irrigated or uses fertilizer, respectively.

	N	Mean	St. Dev.	Min	Max
Household Head					
Female (1 = yes)	984	0.287	0.452	0	1
Age (years)	984	52.625	14.269	20	95
Married (1 = yes)	984	0.854	0.354	0	1
Read French (1 = yes)	983	0.314	0.464	0	1
Write French (1 = yes)	983	0.306	0.461	0	1
Formal School (1 = yes)	983	0.304	0.460	0	1
Household					
Household Size (persons)	984	10.643	6.675	1	58
Household Farm Labor (person days)	384	388.672	462.713	0	2909
Hire Outside Labor (1 = yes)	384	0.430	0.496	0	1
Outside Labor (person days)	394	23.388	55.696	0	348
Rice (1 = yes)	384	0.273	0.446	0	1
Millet (1 = yes)	384	0.242	0.429	0	1
Cowpea (1 = yes)	384	0.474	0.500	0	1
Peanut (1 = yes)	384	0.466	0.500	0	1
Irrigation (1 = yes)	384	0.378	0.485	0	1
Fertilizer (1 = yes)	378	0.458	0.499	0	1

Table S3. Estimated expenditure shares. Estimated expenditure shares from the Harmonized Survey on Household Living Standards in Senegal collected in 2018 and 2019. We classified goods according to three categories: food, health, and household goods where household goods captured goods that did not clearly fit into food or health. We then aggregated annual expenditure for each of the goods in these categories. Some expenditures recorded in the survey were excluded, therefore the totals may not add up to 1.[‡‡] Fewer households report cash health expenditures, so we take these expenditure share estimates as a lower bound when calibrating the household's utility function focusing on the expenditure share estimates for food and household goods.

	N	Mean	St. Dev.	Min	Max
Food Expenditure Share	7156	0.539	0.131	0.027	0.941
Household Good Expenditure Share	7156	0.313	0.126	0.007	0.971
Health Expenditure Share	6035	0.036	0.052	0	0.798

[‡‡] We exclude alcohol and tobacco purchases. Since we abstract away from the land market, we exclude any payments for land or housing.

Table S4. Estimated factor cost shares. Estimated factor cost shares from the Harmonized Survey on Household Living Standards in Senegal collected in 2018 and 2019. We measure land in hectares and then valued land using the rental price of 120,000 FCFA per hectare as reported in the Saint Louis region. We then calculated a household's total labor days on each plot by the following tasks: prepping the land, weeding, and harvesting. We include both family and hired labor and then calculate total labor by adding up all the labor days on each of the family's plots including all three tasks. We then use the median adult male harvesting wage in each region as the value of each day of labor to calculate the total cost of labor. Inorganic fertilizer includes urea, NPK, and phosphates and is measured in kgs. We use the median regional price for each type of inorganic fertilizer when calculating the factor cost. Compost is also measured in kgs. As with inorganic fertilizer, we use the median regional price for animal compost to calculate the factor cost. All carts and sacs are assumed to be 50 kg of fertilizer or animal compost.

	N	Mean	St. Dev.	Min	Max
Land Factor Cost Share	2892	0.416	0.257	0	1
Labor Factor Cost Share	2892	0.529	0.265	0	0.999
Inorganic Fertilizer Factor Cost Share	2892	0.037	0.091	0	0.990
Compost Factor Cost Share	1277	0.040	0.084	0	1

Table S5. Parameters for the household model. The θ parameters for the utility function are based on household expenditure share estimates from the Saint Louis and Louga regions in the Harmonized Survey on Household Living Standards reported in table S3. We round the expenditure share estimates for food and household goods and then scale the parameters on health status and leisure so that the sum of all θ's adds up to one. The parameter h_f is taken from Pitt and colleague's[19] estimate of the relationship between caloric intake and health. We scale the estimate to fit our measure of calories in one kg of rice which is the unit of food in the model. The α parameters for the food production function are based off of factor cost share estimates from the Saint Louis and Louga regions in the Harmonized Survey on Household Living Standards reported in table S4. We round the factor cost share estimates so that the α's add up to one. The substitution parameter ϕ is calibrated to achieve fertilizer use levels consistent with the Senegalese context. The mass loss during compost, modeled by the parameter ω, is based on the range of estimates in Şevik and colleagues[27] and calibrated to achieve fertilizer use consistent with the Senegalese context. The parameters β_v and $\gamma 1$ are estimated from data on vegetation removal done in Rohr and colleagues[11] and reported in SI Appendix Text S3. The price of food comes from Senegalese price reports released by ANSD and the price of fertilizer is consistent with the Harmonized Survey on Household Living Standards and calibrated to achieve stability in the simulations. The price of the household good is calibrated to capture the value of many possible consumption goods the household purchases which are more expensive than food.

Parameter	Description	Value
θ_f	Utility function coefficient on food	0.55
θ_g	Utility function coefficient on household goods	0.3
θ_h	Utility function coefficient on health status	0.1
θ_l	Utility function coefficient on leisure	0.05
h_f	Coefficient on food consumption in health status function	0.000384
α_d	Coefficient on land in food production	0.4
α_l	Coefficient on labor in food production	0.5
α_u	Coefficient on fertilizer in food production	0.05
α_v	Coefficient on vegetation in food production	0.05
ω	Vegetation retained in composting	0.6
ϕ	Substitution parameter	0.3
β_v	Coefficient for harvesting vegetation	14.4942
$\gamma 1$	Exponent on labor in harvesting vegetation	0.2595
p_f	Price of food	290 FCFA
p_h	Price of household good	500 FCFA
p_u	Price of fertilizer	300 FCFA

Table S6. Parameters for the disease ecology model. The parameters β_2, μ_4, λ_2, M_0, ϵ, and k are from Gao and colleagues.[17] The parameters Λ_2, μ_2, and δ_2 are calibrated to achieve a stable snail population throughout the simulations. The parameters λ_1 and μ_3 are calibrated to achieve a stable miracidia population throughout the simulations. The parameters β_1 and α_1 are calibrated to achieve stable infection rates in humans consistent with the 25% infection rate from data collected by Rohr and colleagues.[11] The parameters K and χ are estimated from data collected by Rohr and colleagues.[11] The parameters r, ρ, and $n0$ are calibrated to fit the high growth rate of vegetation observed in the Senegalese context and to adequately capture the effect of fertilizer runoff on vegetation growth. η is calibrated to deworming every four years.

Parameter	Description	Value
r	Vegetation growth rate	0.05
K	Vegetation carrying capacity	28,906.5 kg
ρ	Effect of fertilizer on vegetation growth	0.01
$n0$	Vegetation recolonization rate	0.01
Λ_2	Snail recruitment rate	100
β_1	Contact between cercariae and humans	1.766×10^{-8}
β_2	Probability of snail infection from miracidia	0.615
μ_2	Snail natural mortality rate	0.008
μ_3	Miracidial mortality rate	2.5
μ_4	Cercarial mortality rate	0.004
δ_2	Snail death rate from infection	0.0004012
λ_1	Hatching rate of miracidia	50
λ_2	Cercarial emergence rate	2.6
α_1	Saturation coefficient for cercarial infectivity	0.8×10^{-8}
M_0	Contact rate between miracidia and snails	1.00×10^6
ϵ	Saturation coefficient for miracidial infectivity	0.30
χ	Snail death rate from vegetation removal	0.02842
k	Eggs released per infected human	300
η	Treatment rate of infected humans	0.00068

Table S7. Starting values of the disease ecology populations. Average household size begins at the nearest whole number with easy division into 4 of 10 based on the average household size in the Saint Louis and Louga region from the Harmonized Survey on Household Living Standards in Senegal, 2018-2019. Infected and susceptible humans were then calculated based on the average infection prevalence of *S. mansoni* in the infection data from Rohr and colleagues.[11] All other parameters were calibrated to be consistent with the human infection data.

Parameter	Description	Value
N_0	Starting amount of vegetation	28,906.5 kg
S_1	Susceptible humans	7.5
I_1	Infected humans	2.5
S_2	Susceptible snails	200
I_2	Infected snails	12,300
M	Miracidia	15,000
P	Cercariae	130,000

Table S8. Vegetation production function estimates. Estimates of the vegetation production function in equation 19. Huber-White robust standard errors in parentheses. * p < 0.1, ** p < 0.05, *** p < 0.01

	Log(kg of vegetation)
Log(person days)	0.260***
	(0.0581)
Constant	2.674***
	(0.141)
N	92
Adj. R^2	0.208

Table S9. Parameters for the disease ecology model in Gao and colleagues.[17] Parameter values are taken directly from Gao and colleagues[17] and reported here.

Parameter	Description	Value
Λ_2	Snail recruitment rate	200 d^{-1}
β_1	Contact between cercariae and humans	0.406×10^{-8}
β_2	Probability of snail infection from miracidia	0.615
μ_2	Snail natural mortality rate	0.000569
μ_3	Miracidial mortality rate	0.9
μ_4	Cercarial mortality rate	0.004
δ_2	Snail death rate from infection	0.0004012
λ_1	Hatching rate of miracidia	0.00232
λ_2	Cercarial emergence rate	2.6
α_1	Saturation coefficient for cercarial infectivity	0.3×10^{-8}
M_0	Contact rate between miracidia and snails	1.00×10^6
ϵ	Saturation coefficient for miracidial infectivity	0.30
k	Eggs released per infected human	300
η	Treatment rate of infected humans	0.00068

Table S10. Adjusted parameters for the disease ecology model. A value of "Yes" in the modification column reports that the parameter used in the disease ecology model differs from the model reported in Gao and colleagues.[17] Vegetation does not exist in the Gao and colleagues' model so all vegetation parameters are modifications.

Parameter	Description	Value	Modification
r	Vegetation growth rate	0.05	Yes
K	Vegetation carrying capacity	28,906.5 kg	Yes
ρ	Effect of fertilizer on vegetation growth	0.01	Yes
$n0$	Vegetation recolonization rate	0.01	Yes
Λ_2	Snail recruitment rate	100	Yes
β_1	Contact between cercariae and humans	1.766×10^{-8}	Yes
β_2	Probability of snail infection from miracidia	0.615	No
μ_2	Snail natural mortality rate	0.008	Yes
μ_3	Miracidial mortality rate	2.5	Yes
μ_4	Cercarial mortality rate	0.004	No
δ_2	Snail death rate from infection	0.0004012	Yes
λ_1	Hatching rate of miracidia	50	Yes
λ_2	Cercarial emergence rate	2.6	No
α_1	Saturation coefficient for cercarial infectivity	0.8×10^{-8}	Yes
M_0	Contact rate between miracidia and snails	1.00×10^6	No
ϵ	Saturation coefficient for miracidial infectivity	0.30	No
χ	Snail death rate from vegetation removal	0.02842	Yes
k	Eggs released per infected human	300	No
η	Treatment rate of infected humans	0.00068	No

References

1. M. H. Bonds, D. C. Keenan, P. Rohani, J.D. Sachs, Poverty trap formed by the ecology of infectious diseases. *Proceedings of the Royal Society B: Biological Sciences* **277**, 1185-1192 (2010).
2. J-C. Berthélemy, J. Thuilliez, O. Doumbo, J. Gaudart, Malaria and protective behaviours: Is there a malaria trap? *Malaria Journal* **12**, 1-9 (2013).
3. A. Garchitorena A, *et al.*, Economic inequality caused by feedbacks between poverty and the dynamics of a rare tropical disease: The case of Buruli ulcer in sub-Saharan Africa. *Proceedings of the Royal Society B: Biological Sciences* **282**, 20151426 (2015).
4. A. Goenka, L. Liu, Infectious diseases, human capital and economic growth. *Economic Theory* **70**, 1-47 (2020).
5. C. N. Ngonghala, *et al.*, Poverty, disease, and the ecology of complex systems. PLoS Biology **12**, e1001827 (2014).
6. C. N. Ngonghala, *et al.*, General ecological models for human subsistence, health and poverty. *Nature Ecology & Evolution* **1**, 1153–1159 (2017).
7. M. M. Pluciński, C. N. Ngonghala, M. H. Bonds, Health safety nets can break cycles of poverty and disease: A stochastic ecological model. *Journal of the Royal Society Interface* **8**,1796-1803 (2011).
8. M. M. Pluciński, C. N. Ngonghala, W. M. Getz, M. H. Bonds, Clusters of poverty and disease emerge from feedbacks on an epidemiological network. *Journal of The Royal Society Interface* **10**, 20120656 (2013).
9. O. Varis, V. Stucki, S. Fraboulet-Jussila, The Senegal River Case. *Soil & Water,* 1-10 (2006).
10. E. Léger, *et al.*, Prevalence and distribution of schistosomiasis in human, livestock, and snail populations in northern Senegal: A One Health epidemiological study of a multi-host system. *The Lancet Planetary Health* **4**, e330-e342 (2020).
11. J. R. Rohr, *et al.*, A planetary health innovation for disease, food and water challenges in Africa. *Nature* **619**, 782–787 (2023).
12. WAEMU Commission, Harmonized Survey on Households Living Standards, Senegal 2018-2019. Ref. SEN_2018_**EHCVM**_v02_M. 2018; Dataset downloaded from www.microdata.worldbank.org on September 23, 2022.
13. J. R. Rohr, *et al.*, Emerging human infectious diseases and the links to global food production. *Nature Sustainability* **2**, 445–456 (2019).
14. C. M. Hoover, *et al.*, Effects of agrochemical pollution on schistosomiasis transmission: A systematic review and modelling analysis. *The Lancet Planetary Health* **4**: e280-e291 (2020).
15. B. Gryseels, K. Polman, J. Clerinx, L. Kestens, Human schistosomiasis. *The Lancet* **368**, 1106–1118 (2006).
16. C. J. Haggerty, *et al.*, Aquatic macrophytes and macroinvertebrate predators affect densities of snail hosts and local production of schistosome cercariae that cause human schistosomiasis. *PLoS Neglected Tropical Diseases* **14**, e0008417 (2020).
17. S. Gao, Y. Liu, Y. Luo, D. Xie, Control problems of a mathematical model for schistosomiasis transmission dynamics. *Nonlinear Dynamics* **63**, 503–512 (2011).
18. A. D. Foster, M. R. Rosenzweig, A test for moral hazard in the labor market: Contractual arrangements, effort, and health. *Review of Economics and Statistics*, 213-227 (1994).
19. M. M. Pitt, M. R. Rosenzweig, M. N. Hassan, Productivity, health, and inequality in the intrahousehold distribution of food in low-income countries. *American Economic Review*, 1139-1156 (1990).
20. E. B. McCullough, Labor productivity and employment gaps in Sub-Saharan Africa. *Food Policy* **67**, 133-152 (2017).
21. ANSD, Bulletin Mensuel des Statistiques Economiques. Agence National de la Statistique et de la Démographie de la République du Sénégal. 2018; Accessed online from http://www.ansd.sn/index.php?option=com_ansd&view=titrepublication&id=9&Itemid=287 on May 20, 2020.

22. M. Fafchamps, Sequential labor decisions under uncertainty: An estimable household model of west-African farmers. *Econometrica* **61**, 1173-1197 (1993).
23. B. Dillon, Private Information and Dynamic Risk. *Working Paper* (2017).
24. K. H. Nguyen, *et al.*, Interventions can shift the thermal optimum for parasitic disease transmission. *Proceedings of the National Academy of Sciences* **118**, e2017537118 (2021).
25. M. A. Verjee, Schistosomiasis: Still a cause of significant morbidity and mortality. *Research and Reports in Tropical Medicine* **10**, 153 (2019).
26. J. R. Rohr *et al.*, Data and Code for "A planetary health innovation for disease, food, and water challenges in Africa" [Data set]. Zenodo. https://doi.org/10.5281/zenodo.7765059
27. F. Şevik, İ. Tosun, K. Ekinci, The effect of FAS and C/N ratios on co-composting of sewage sludge, dairy manure and tomato stalks. *Waste Management* **80**, 450-456 (2018).